



# Preclinical Pharmacokinetics and Safety of Intravenous RTD-1

A. Young J. Park,<sup>a</sup> Dat Q. Tran,<sup>b,c</sup>  Justin B. Schaal,<sup>b</sup> Mengxi Wang,<sup>a</sup> Michael E. Selsted,<sup>b,c</sup>  Paul M. Beringer<sup>a</sup>

<sup>a</sup>Department of Clinical Pharmacy, School of Pharmacy, University of Southern California, Los Angeles, California, USA

<sup>b</sup>Department of Pathology and Laboratory Medicine, Keck School of Medicine, University of Southern California, Los Angeles, California, USA

<sup>c</sup>Oryn Therapeutics, Vacaville, California, USA

**ABSTRACT** Severe illness caused by coronavirus disease 2019 (COVID-19) is characterized by an overexuberant inflammatory response resulting in acute respiratory distress syndrome (ARDS) and progressive respiratory failure (A. Gupta, M. V. Madhavan, K. Sehgal, N. Nair, et al., *Nat Med* 26:1017–1032, 2020, <https://doi.org/10.1038/s41591-020-0968-3>). Rhesus theta ( $\theta$ ) defensin-1 (RTD-1) is a macrocyclic host defense peptide exhibiting antimicrobial and immunomodulatory activities. RTD-1 treatment significantly improved survival in murine models of a severe acute respiratory syndrome (SARS-CoV-1) and endotoxin-induced acute lung injury (ALI) (C. L. Wohlford-Lenane, D. K. Meyerholz, S. Perlman, H. Zhou, et al., *J Virol* 83:11385–11390, 2009, <https://doi.org/10.1128/JVI.01363-09>; J. G. Jayne, T. J. Bensman, J. B. Schaal, A. Y. J. Park, et al., *Am J Respir Cell Mol Biol* 58:310–319, 2018, <https://doi.org/10.1165/rcmb.2016-0428OC>). This investigation aimed to characterize the preclinical pharmacokinetics (PK) and safety of intravenous (i.v.) RTD-1. Based on the lack of adverse findings, the no observed adverse effect level (NOAEL) was established at 10 mg/kg/day in rats and 15 mg/kg/day in monkeys. Analysis of single ascending dose studies in both species revealed greater-than-dose-proportional increases in the area under the curve extrapolated to infinity ( $AUC_{0-\infty}$ ) (e.g., 8-fold increase from 5 mg/kg to 20 mg/kg in rats) suggestive of nonlinear PK. The volume of distribution at steady state ( $V_{ss}$ ) ranged between 550 and 1,461 mL/kg, indicating extensive tissue distribution, which was validated in a biodistribution study of [<sup>14</sup>C]RTD-1 in rats. Based on interspecies allometric scaling, the predicted human clearance and  $V_{ss}$  are 6.48 L/h and 28.0 L, respectively, for an adult (70 kg). To achieve plasma exposures associated with therapeutic efficacy established in a murine model of ALI, the estimated human equivalent dose (HED) is between 0.36 and 0.83 mg/kg/day. The excellent safety profile demonstrated in these studies and the efficacy observed in the murine models support the clinical investigation of RTD-1 for treatment of COVID-19 or other pulmonary inflammatory diseases.

**KEYWORDS** COVID-19, host defense peptide, pharmacokinetics, rhesus theta defensin, safety

The coronavirus disease 2019 (COVID-19) is caused by the novel coronavirus, severe acute respiratory syndrome coronavirus 2 (SARS-CoV-2), which is a single, positive-stranded RNA virus that belongs to the  $\beta$  genus of the *Coronaviridae* family. The disease is characterized by acute lung injury (ALI), which can progress to respiratory failure and death (1). In addition, elevated levels of pro-inflammatory cytokines, including interleukin 6 (IL-6), IL-2, granulocyte colony-stimulating factor (G-CSF), IP-10 (CXCL10), monocyte chemoattractant protein 1 (MCP1, CCL2), macrophage inflammatory protein (MIP, CCL3) 1 $\alpha$ , gamma interferon (IFN- $\gamma$ ), and tumor necrosis factor alpha (TNF- $\alpha$ ), are detectable in the blood samples of patients with severe COVID-19 infections, an observation referred to as cytokine storm syndrome (CSS) (4). As such, CSS is a leading cause of mortality in COVID-19 patients. Furthermore, several studies suggest a direct correlation between cytokine storm and lung injury and multiple organ failure (5–7). In the

**Copyright** © 2022 American Society for Microbiology. All Rights Reserved.

Address correspondence to Michael E. Selsted, selsted@med.usc.edu, or Paul M. Beringer, beringer@usc.edu.

The authors declare a conflict of interest. M.E.S. (co-founder, chief scientific officer) and D.Q.T. (scientific director) hold part-time appointments with Oryn Therapeutics, LLC, which has licensed theta defensin technologies for commercial development. P.M.B. is a consultant to Oryn Therapeutics, LLC.

**Received** 3 November 2021

**Returned for modification** 3 December 2021

**Accepted** 7 January 2022

**Accepted manuscript posted online**

18 January 2022

**Published** 15 March 2022

RECOVERY trial, in which COVID-19 patients were randomized to receive dexamethasone or placebo, the use of dexamethasone reduced the incidence of death in patients receiving either invasive mechanical ventilation or oxygen alone, highlighting the role of anti-inflammatory therapies in the treatment of COVID-19 (8).

Rhesus theta ( $\theta$ ) defensin-1 (RTD-1) is a host defense peptide that possesses both antimicrobial and immunomodulatory properties. *In vitro* studies have demonstrated its activities against several microbes, including *Pseudomonas aeruginosa*, *Staphylococcus aureus*, *Escherichia coli*, *Candida albicans*, and HIV-1 (9–12). One of the mechanisms in which RTD-1 exerts its immunomodulatory activity is via the inhibition of mitogen-activated protein kinase (MAPK) and NF- $\kappa$ B signaling pathways through the upregulation of AKT phosphorylation, leading to a reduction in the production of proinflammatory cytokines and chemokines (13). The inhibition of NF- $\kappa$ B activation and the downstream genes lead to a reduction in airway neutrophil recruitment and adhesion, as well as neutrophil activation (3). Additionally, *in vitro* experiments have revealed that RTD-1 acts as a noncompetitive inhibitor of the TNF- $\alpha$ -converting enzyme (TACE, ADAM17) (14). The anti-inflammatory activities of RTD-1 were discovered during investigations of the efficacy of intranasal RTD-1 in a murine model of SARS-CoV lung disease, which was responsible for the outbreak of SARS in 2002 (2), and in rodent models of polymicrobial sepsis (15), systemic candidiasis (12), and rheumatoid arthritis (16, 17). In the SARS-CoV model, prophylactic treatment of RTD-1 led to a significant improvement in the survival of infected mice without any changes in the viral load, suggesting that the beneficial effect of RTD-1 is likely derived from its immunomodulatory activities. In the murine model of LPS-induced ALI, subcutaneous administration of RTD-1 at 5 and 25 mg/kg led to attenuation of the airway inflammatory response through the inhibition of proinflammatory cytokine production, peroxidase activity, and neutrophil recruitment and protected against lung injury (3).

This report summarizes the analyses from several studies including two Good Laboratory Practice (GLP) studies undertaken in rodent and nonrodent species and a non-GLP dose range-finding study in cynomolgus monkeys to assess the safety and pharmacokinetics of single- and repeat-dose intravenous (i.v.) RTD-1 administration. The preclinical experiments were conducted to determine the safety and first-in-human (FIH) dosing in preparation for clinical trials of i.v. RTD-1 for treatment of COVID-19.

## RESULTS

**Pharmacokinetics. (i) Mice.** The mean plasma concentration-time profile after single-dose administration in mice is shown in Fig. 1A, and the corresponding pharmacokinetic (PK) parameters calculated by noncompartmental analysis (NCA) are given in Table 1. Due to terminal blood collection from each mouse, a pooled PK result was generated. After single i.v. bolus administration, RTD-1 displayed a biphasic profile, with a relatively short distribution phase followed by a longer elimination phase with a half-life of 6.05 h.

**(ii) Rats.** The mean plasma concentration-time profiles in rats following single-dose (5, 10, or 20 mg/kg) or multiple-dose (5 or 10 mg/kg/day) administrations are depicted in Fig. 1B and Fig. 2A and B, respectively, and the corresponding PK parameters are summarized in Tables 1 and 2. Of the total 180 infusions from 36 rats, five infusions deviated more than 10% from the intended 20-min infusion. However, these deviations did not occur on blood PK sampling days and therefore did not influence the PK analysis. Due to sparsely sampled data per rat, a pooled PK result was generated in WinNonlin. Plasma levels of RTD-1 were undetectable during the recovery period (day 25) in all rats, except for one female rat that received 10 mg/kg, which had a concentration of 12.5 ng/mL. Early removal of the rats in the 20-mg/kg group precluded the PK analysis with repeat dosing at this dose level. The maximum observed concentration in plasma ( $C_{max}$ ) was slightly higher in female than male rats, but the differences did not reach statistical significance. While both the  $C_{max}$  and the area under the concentration-time curve from 0 h to infinity ( $AUC_{0-\infty}$ ) appeared to increase proportionally

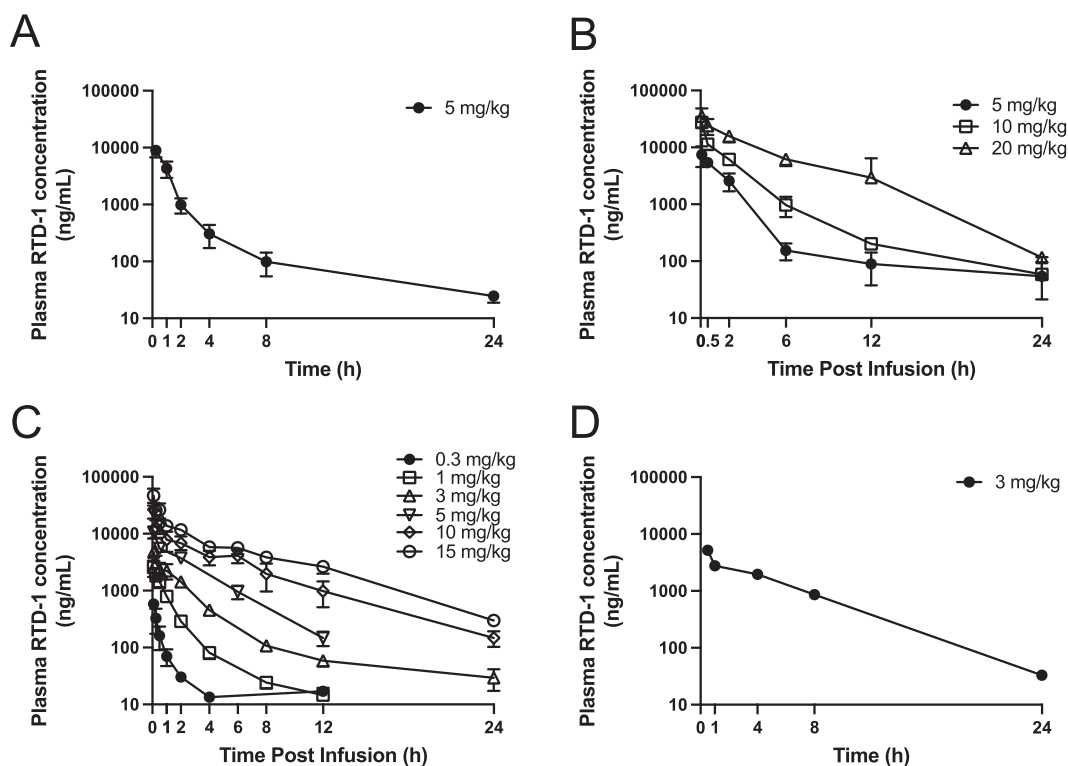


**FIG 1** Mean (standard deviation [SD]) plasma concentration-time profiles of RTD-1 in mice ( $n = 4$ /time point) (A), rats ( $n = 6$ /time point) (B), cynomolgus monkeys ( $n = 2$  to 12/dosing group) (C), and a vervet ( $n = 1$ ) (D) following single-dose i.v. administration.

to the dose based on the 95% confidence interval (CI) of the slope including 1 ( $C_{max}$   $Y = 1.110 \times X + 8.936$  [slope 95% CI, 0.7066 to 1.513],  $R^2 = 0.6803$ ;  $AUC_{0-\infty}$   $Y = 1.543 \times X + 9.448$  [slope 95% CI, 0.4460 to 2.639],  $R^2 = 0.9969$ ), a comprehensive analysis of dose proportionality in rats was limited due to pooled calculations of  $AUC_{0-\infty}$  at each dose level and the relatively narrow range of doses tested. The area under the concentration-time curve to dosing interval ( $AUC_{\tau}$ ) values on day 7 were slightly lower (22% and 19% for the 5- and 10-mg/kg/day groups, respectively) than their  $AUC_{0-\infty}$  values on day 1, indicating no significant drug accumulation.

**(iii) Cynomolgus monkeys.** The mean plasma concentration-time profiles in cynomolgus monkeys following single- or multiple-dose administrations are illustrated in

**TABLE 1** Single-dose pharmacokinetics in mice, rats, cynomolgus monkeys, and vervet

Parameter <sup>a</sup>	Value for:			
	Mice	Rats	Cynomolgus monkeys <sup>c</sup>	Vervet
$n$	4/time point	12	6	1
Dose (mg/kg)	5	5	5	3
$C_{max}$ (ng/mL)	8,919 (1,088) <sup>b</sup>	7,468 (1,202) <sup>b</sup>	10,700 (2,455)	5,193
$\lambda_z$ ( $h^{-1}$ )	0.114	0.056	0.323 (0.016)	0.204
$AUC_{\tau}$ (ng · h/mL)	12,282	14,956	27,160 (4,286)	21,949
$AUC_{0-\infty}$ (ng · h/mL) <sup>d</sup>	12,497	15,948	27,176 (4,292)	22,110
CL (mL/h/kg)	400	334	188 (29.2)	136
MRT (h)	2.62	4.37	2.94 (0.15)	4.71
$V_{ss}$ (mL/kg)	1,048	1,461	550 (74.6)	639

<sup>a</sup> $C_{max}$ , maximum observed plasma concentration;  $\lambda_z$ , terminal elimination rate constant;  $AUC_{\tau}$ , area under the concentration-time curve to the dosing interval (24 h);  $AUC_{0-\infty}$ , area under the concentration-time curve extrapolated to infinity; CL, clearance; MRT, mean residence time;  $V_{ss}$ , volume of distribution at steady state.

<sup>b</sup>Data are estimates (standard error).

<sup>c</sup>Mean (SD).

<sup>d</sup>A target  $AUC_{0-\infty}$  between 3,869 and 9,001 ng · h/mL required for therapeutic efficacy was previously established in a murine model of LPS-induced ALI.

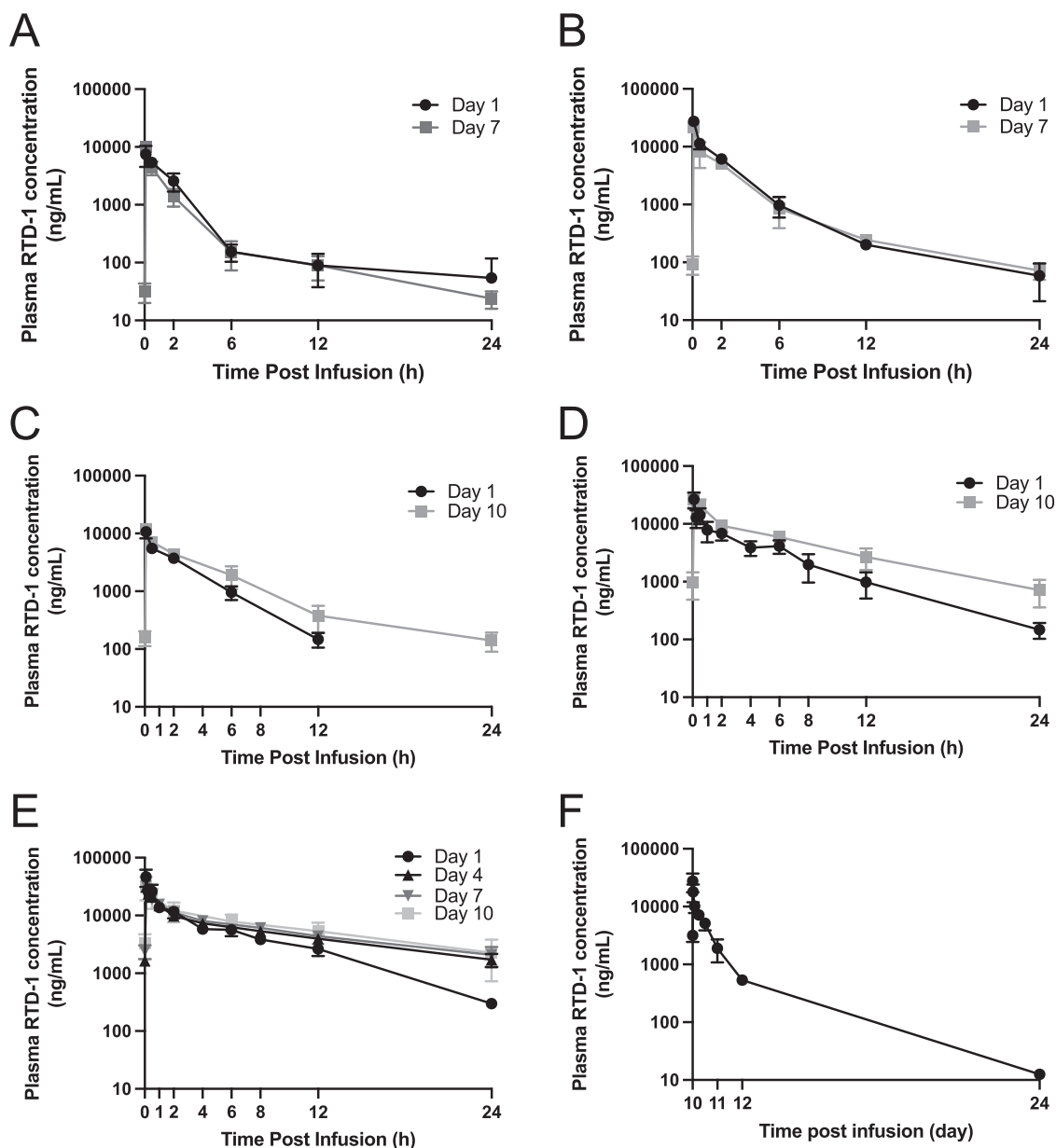


**FIG 2** Mean (SD) plasma concentration versus time profiles following repeated i.v. administration of RTD-1 in rats at 5 mg/kg/day (A) and 10 mg/kg/day (B), in cynomolgus monkeys at 5 mg/kg/day (C), 10 mg/kg/day (D), and 15 mg/kg/day (E), and in the recovery group after the 10th dose (15 mg/kg/day,  $n = 4$ ) (F).

Fig. 1C and 2C to F, respectively. The corresponding PK parameters calculated by NCA are outlined in Tables 1 and 3. Of the total 233 infusions from 24 cynomolgus monkeys, four infusions deviated more than 10% from the intended 1-h infusion. However, these deviations did not occur on blood PK sampling days and therefore did not influence the PK analysis. Data from two separate studies involving single and multiple dosing in cynomolgus monkeys were combined in this analysis. Overall, concentration-time profiles displayed a biphasic pattern, with a prolonged elimination phase at higher doses. Plasma concentrations of RTD-1 after a single dose of 0.3 or 1 mg/kg were detectable up to 12 h post-end of infusion. In the GLP-compliant 10-day toxicokinetic (TK) study, all animals received 10 i.v. doses except for one female monkey in the 15-mg/kg/day group, which received a total of 9 doses due to issues with venous access. Extended sampling with cynomolgus monkeys assigned to the recovery group (15 mg/kg/day) revealed that plasma levels of RTD-1 were quantifiable on day 12 (537 ng/mL) and day

**TABLE 2** Multiple-ascending-dose pharmacokinetics of i.v. RTD-1 in rats

Parameter <sup>a</sup>	Value <sup>b</sup> at indicated dose and day				
	5 mg/kg		10 mg/kg		20 mg/kg
	Day 1	Day 7	Day 1	Day 7	Day 1
<i>n</i>	12	12	12	12	12
<i>C</i> <sub>max</sub> (ng/mL)	7,468 (1,202)*#	10,137 (688)	27,533 (1,419)*	21,850 (759)	35,400 (5,350)#
$\lambda_z$ (h <sup>-1</sup> )	0.056	0.104	0.148	0.133	0.221
AUC <sub>r</sub> (ng · h/mL)	14,956	12,468	41,669	34,121	126,860
AUC <sub>0-∞</sub> (ng · h/mL) <sup>c</sup>	15,948	12,704	42,085	34,688	127,386
CL (mL/h/kg)	334	401	240	293	157
MRT (h)	4.37	2.92	2.88	3.45	4.81
<i>V</i> <sub>ss</sub> (mL/kg)	1,461	1,173	691	1,011	756

<sup>a</sup>*C*<sub>max</sub>, maximum observed plasma concentration;  $\lambda_z$ , terminal elimination rate constant; AUC<sub>r</sub>, area under the concentration-time curve to dosing interval (24 h); AUC<sub>0-∞</sub>, area under the concentration-time curve extrapolated to infinity; CL, clearance; MRT, mean residence time; *V*<sub>ss</sub>, volume of distribution at steady state.

<sup>b</sup>Data are estimates (standard error). Symbols (\*, #) denote statistically significant differences between matching groups (*P* < 0.05).

<sup>c</sup>A target AUC<sub>0-∞</sub> between 3,869 and 9,001 ng · h/mL required for therapeutic efficacy was previously established in a murine model of LPS-induced ALI.

24 (12.5 ng/mL), indicating that RTD-1 exhibits a long terminal half-life (Fig. 2F). The average terminal half-life in the recovery animals was 47.2 h compared to 9.53 h in the main group with the shorter sampling period. The *C*<sub>max</sub> and AUC<sub>0-∞</sub> were slightly higher in males than females, but the differences did not reach statistical significance. A detailed assessment of dose proportionality in cynomolgus monkeys administered a single i.v. dose ranging from 0.3 to 15 mg/kg revealed that both *C*<sub>max</sub> and AUC<sub>0-∞</sub> increased more than dose proportionally (Fig. 3). Specifically, the AUC<sub>0-∞</sub> was dose proportional at lower doses (0.3 to 3 mg/kg) but began to deviate from dose proportionality at higher doses (≥5 mg/kg) (data not shown). Dose proportionality assessment at steady state demonstrated that while the *C*<sub>max</sub> increased dose proportionally (*C*<sub>max</sub>,  $Y = 0.9553 \times X + 6.805$  [slope 95% CI, 0.5573 to 1.353, *R*<sup>2</sup> = 0.5705]), the AUC<sub>r</sub> increased more than dose proportionally (AUC<sub>r</sub>,  $Y = 1.422 \times X + 6.745$  [slope 95% CI, 1.072 to 1.772, *R*<sup>2</sup> = 0.7916]). However, these results were limited due to the narrow range of doses examined. Comparisons of AUCs after a single dose (day 1) and repeat dose administrations (day 10) revealed statistically significant accumulations at 5 and 10 mg/kg/day, yielding approximately 1.4- and 1.5-fold-higher mean AUC<sub>r</sub> than mean AUC<sub>0-∞</sub> on day 1 for 5- and 10-mg/kg/day doses, respectively (5 mg/kg/day, *P* = 0.0229; 10 mg/kg/day, *P* = 0.0103). Although there was a trend toward RTD-1 accumulation at 15 mg/kg/day at a steady state (day 10), the difference did not reach statistical significance (*P* = 0.1879). Statistical analysis was not performed with the PK parameters calculated on days 4 and 7 in the 15-mg/kg/day group due to the small number of animals (*n* = 2).

**(iv) Vervet.** The mean plasma concentration-time profile of RTD-1 in the vervet after a single i.v. bolus administration is shown in Fig. 1D, and the PK parameters are presented in Table 1. Following the bolus administration, plasma concentrations of RTD-1 declined monoexponentially. However, the plasma concentrations collected after 24 h were below the lower limit of quantification and therefore excluded from the analysis.

**Interspecies allometric scaling.** Overall, linear regression of logarithmically transformed clearance (CL) or volume of distribution at steady state (*V*<sub>ss</sub>) against log-transformed body weight (BW) from the four preclinical species resulted in a reasonable fit, as evidenced by the relatively high *r*<sup>2</sup> (Fig. 4). The allometric scaling equations for CL and *V*<sub>ss</sub> were  $Y = 190.5 \times BW^{0.8302}$  (*r*<sup>2</sup> = 0.7761) and  $Y = 709.6 \times BW^{0.8651}$  (*r*<sup>2</sup> = 0.8918), respectively, which yielded the predicted human CL of 6.48 L/h and *V*<sub>ss</sub> of 28.0 L. Based on the target plasma AUC<sub>0-∞</sub> values of approximately 3,869 and 9,001 ng · h/mL, which were previously established in a murine model of LPS-induced ALI, the estimated human equivalent doses (HED) to reach therapeutic efficacy are between 25.1 and 58.4 mg for a 70-kg individual or between 0.36 and 0.83 mg/kg/day.

**TABLE 3** Single-dose and multiple-ascending-dose pharmacokinetics of i.v. RTD-1 in cynomolgus monkeys

Parameter <sup>a</sup>	Value <sup>b</sup> for indicated dose, day, and no. of monkeys													
	0.3 mg/kg		1 mg/kg		3 mg/kg		5 mg/kg		10 mg/kg		15 mg/kg			
	Day 1 n = 2	Day 1 n = 2	Day 1 n = 2	Day 1 n = 2	Day 1 n = 2	Day 10 n = 6	Day 1 n = 8	Day 10 n = 6	Day 1 n = 8	Day 10 n = 6	Day 1 n = 12	Day 4 n = 2	Day 7 n = 2	Day 10 n = 9
C <sub>max</sub> (ng/mL)	582 (109)	2,560 (820)	4,750 (905)	10,700 (2,455)	11,675 (2,036)	27,333 (7,361)	26,675 (8,240)	27,333 (7,361)	46,458 (15,247)†	31,100 (283)	32,850 (919)	32,233 (13,933)†	32,850 (919)	32,233 (13,933)†
λ <sub>z</sub> (h <sup>-1</sup> )	0.523 (0.119)	0.251 (0.035)	0.078 (0.017)	0.323 (0.016)#	0.157 (0.009)#	0.120 (0.018)*	0.192 (0.034)*	0.120 (0.018)*	0.149 (0.019)†	0.072 (0.020)	0.071 (0.017)	0.078 (0.020)†	0.071 (0.017)	0.078 (0.020)†
AUC <sub>τ</sub> (ng · h/mL)	591 (145)	3,818 (961)	10,334 (2,239)	27,160 (4,286)	38,936 (9,829)	76,083 (23,562)	117,529 (26,077)	138,135 (34,942)	139,595 (2,366)	154,149 (12,406)	173,315 (67,934)	173,315 (67,934)	154,149 (12,406)	173,315 (67,934)
AUC <sub>0-∞</sub> (ng · h/mL) <sup>c</sup>	617 (137)	3,875 (973)	10,740 (2,485)	27,176 (4,292)	39,997 (10,219)	76,820 (23,871)	124,790 (30,604)	142,095 (35,842)	167,061 (16,034)	187,609 (31,623)	212,728 (104,487)	212,728 (104,487)	187,609 (31,623)	212,728 (104,487)
CL (mL/h/kg)	498 (111)	266 (66.9)	287 (66.4)	188 (29.2)#	136 (36.5)#	88.5 (18.5)*	143 (48.2)*	88.5 (18.5)*	114 (25.7)	107 (1.82)	97.6 (7.86)	103.53.0	97.6 (7.86)	103.53.0
MRT <sub>inf</sub> (h)	1.24 (0.16)	1.82 (0.07)	4.30 (0.60)	2.94 (0.15)	4.84 (0.57)	7.20 (1.04)	4.40 (0.50)	7.20 (1.04)	5.48 (0.76)	11.8 (2.46)	12.3 (3.08)	12.0 (3.33)	12.3 (3.08)	12.0 (3.33)
V <sub>ss</sub> (mL/kg)	626 (218)	486 (139)	1,215 (112)	550 (74.6)	645 (123)	624 (88.2)	629 (231)	624 (88.2)	629 (176)†	1,263 (242)	1,193 (204)	1,139 (411)†	1,193 (204)	1,139 (411)†

<sup>a</sup>C<sub>max</sub>, maximum observed plasma concentration; λ<sub>z</sub>, terminal elimination rate constant; AUC<sub>τ</sub>, area under the concentration-time curve to dosing interval (24 h); AUC<sub>0-∞</sub>, area under the concentration-time curve extrapolated to infinity; CL, clearance; MRT, mean residence time; V<sub>ss</sub>, volume of distribution at steady state.

<sup>b</sup>Data are mean (SD). Symbols (#, \*, †) denote statistically significant differences within the dosing group between day 1 and day 10 (P < 0.05).

<sup>c</sup>A target AUC<sub>0-∞</sub> between 3,869 and 9,001 ng · h/mL required for therapeutic efficacy was previously established in a murine model of LPS-induced ALI.

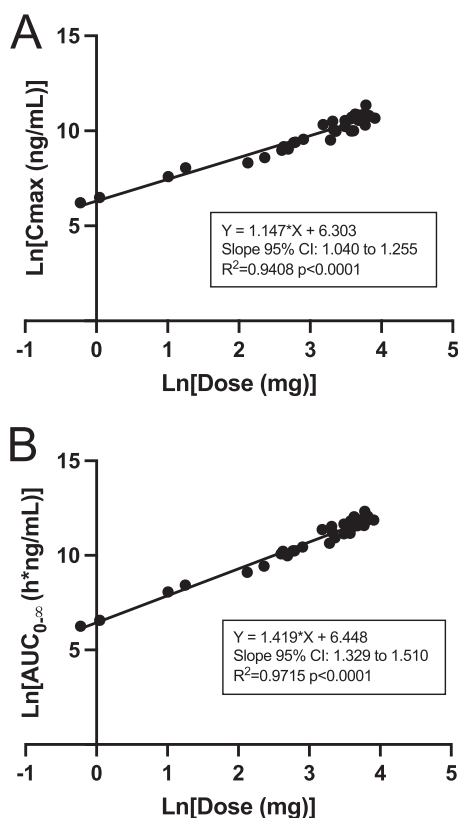


**FIG 3** Assessment of dose proportionality of  $C_{max}$  (A) and  $AUC_{0-\infty}$  (B) in cynomolgus monkeys following a single-dose administration of RTD-1 (0.3, 1, 3, 10, or 15 mg/kg).

**Biodistribution.** The biodistribution study was undertaken to determine the patterns of distribution and potential routes of elimination of RTD-1 in rats after a single-dose i.v. administration of [<sup>14</sup>C]RTD-1 equivalent to 5 mg/kg. Widespread distribution of [<sup>14</sup>C]RTD-1 was observed at 1 h, with the highest density measured in the liver, followed by the kidney (see Table S5 in the supplemental material). At 1 h, there was a trace amount of <sup>14</sup>C counts measured in the urine, skin, leg muscle, eyes, and brain. After 24 h, the density of <sup>14</sup>C counts in the tissues and organs decreased relative to counts detected at 1 h, except for those in the urine. The <sup>14</sup>C counts in urine increased from trace amounts at 1 h to 8.5% after 24 h. Moreover, approximately 4% of the [<sup>14</sup>C] RTD-1 dose administered was recovered in the feces at 24 h, suggesting that the major route of elimination is urinary, followed by biliary excretion.

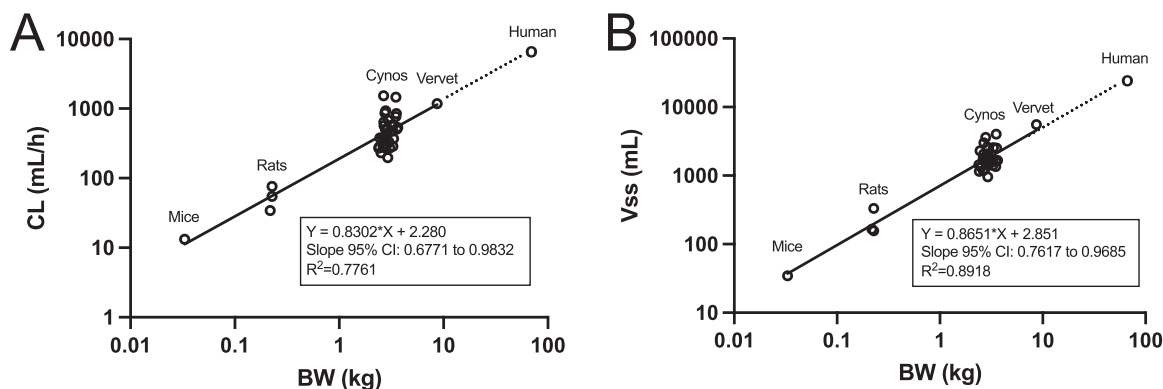


**FIG 4** Interspecies allometric correlation. The plot was created based on the results of RTD-1 single-dose PK studies. The dashed line represents the predicted CL (6.48 L/h) (A) or  $V_{ss}$  (28.0 L) (B) for an adult (70 kg).

**Safety. (i) Rats.** In general, single doses up to 10 mg/kg were well tolerated in male and female rats. During the study, mortality was observed in a total of 7 rats. Specifically, 1 out of 18 female rats in the placebo group was found dead on day 6, and another 1 out of 16 female rats in the 5-mg/kg/day dose group was found dead on day 15 of the study. However, the mortality of the female rat in the 5-mg/kg/day group was determined to be unrelated to RTD-1 treatment due to minimal clinical manifestations until the day of death and the timing of the event. Additionally, a single i.v. administration of 20 mg/kg RTD-1 led to acute, treatment-related mortality in 5 out of 12 rats on day 1. Of the five rats, three male rats were found dead, and one male and one female rat were euthanized due to moribund conditions.

Following once daily i.v. infusion of RTD-1 (5 and 10 mg/kg/day), treatment-related clinical signs, such as muscle fasciculation, lethargy, swollen nose, chin, and/or cheeks, swollen front limbs, reluctance to walk and/or stand, hypoactivity, ataxia, and increased respiration, were noted throughout the study at both dose levels but were temporary and resolved during the recovery period. There were no significant changes in body weight in rats except for those in the 20-mg/kg dosing group, where significant decreases in body weights were recorded in both male and female rats (data not shown). Food consumption was not significantly affected by treatment administration in rats at any dose level. Due to the unexpected mortality and adverse treatment-related clinical observations at 20 mg/kg, the study in this dosing group was prematurely terminated, and the remaining rats were euthanized before their scheduled administration on day 1 or 2. Adverse clinical observations associated with mortalities observed at the lowest observed adverse effect level (LOAEL) included cold to touch, lying on the side, abnormal body color (pale), inability to walk, extreme dehydration, tremors, and labored respiration.

No treatment-related changes in hematological parameters were observed in male and female rats at 5 mg/kg/day at the end of treatment (day 8) (Table 4). At the end of recovery, red blood cell (RBC) volume distribution width (RDW) was significantly elevated in female rats at 5 mg/kg/day and was outside of the historical control range (HCR) for female Sprague-Dawley rats (data not shown). At 10 mg/kg/day, a significant decrease in absolute reticulocytes in male rats treated with 10 mg/kg/day was observed at the end of treatment. However, this value was within the HCR for male Sprague-Dawley rats of this age (18). In female rats, there were significant increases in white blood cell (WBC) count and absolute lymphocytes and monocytes at the end of treatment in comparison to controls. However, these increases were not dose dependent and the changes were reversible by the end of the recovery period (data not shown). At the end of recovery, mean cell hemoglobin (MCH) and mean cell hemoglobin concentration (MCHC) increased modestly in male rats compared to the controls, but the values remained within the reference range for male rats of similar age. At 20 mg/kg, counts of WBC relative and absolute neutrophils, relative and absolute monocytes, and relative and absolute large unclassified cells (LUC) were significantly elevated in male rats, while relative lymphocytes, relative and absolute eosinophils, and platelet count significantly decreased on day 2 compared to controls at the end of treatment. The relative and absolute neutrophil, relative lymphocyte, and relative and absolute monocyte values were outside of the HCR for male rats. In female rats, there were significant increases in absolute reticulocytes and monocytes, while significant decreases in relative and absolute eosinophils were observed on day 2 (interim euthanasia) in comparison with controls at the end of treatment. Due to the premature termination of the study in the 20-mg/kg group, the reversibility of the alterations in these parameters could not be determined. However, regardless of statistical significance, these changes remained within the HCR for female rats. The histopathological examinations of bone marrow samples from sternum and femur samples were within normal limits, except for a mild fracture observed in a male rat at 10 mg/kg/day.

There were no significant treatment-induced abnormalities in serum biochemical parameters at the end of treatment in male and female rats that received 5 or 10 mg/kg/day

**TABLE 4** Hematological results of male and female rats at the end of treatment

Parameter <sup>a</sup>	Value <sup>b</sup> for rats at indicated dose							
	Male			Female				
	0 mg/kg	5 mg/kg	10 mg/kg	20 mg/kg <sup>c</sup>	0 mg/kg	5 mg/kg	10 mg/kg	20 mg/kg <sup>c</sup>
RBC (10 <sup>6</sup> /mm <sup>3</sup> )	6.69 (0.64)	7.06 (0.23)	7.06 (0.38)	6.04 (0.47) <sup>d,e</sup>	6.92 (0.36)	6.88 (0.33)	7.21 (0.40)	7.63 (2.19)
Hemoglobin (g/dL)	13.80 (0.85)	14.10 (0.98)	14.20 (0.65)	12.10 (1.00) <sup>d,e</sup>	13.15 (0.93)	13.50 (1.00)	13.70 (0.38)	15.15 (4.58)
Hematocrits (%)	42.55 (2.90)	43.75 (1.73)	43.65 (1.20)	37.30 (3.70) <sup>d,e</sup>	40.75 (2.15)	40.50 (1.90)	41.15 (1.83)	46.85 (14.28)
MCV (fL)	62.40 (3.05)	61.75 (2.90)	62.60 (3.05)	62.50 (2.10)	57.95 (2.72)	57.90 (2.80)	57.30 (2.43)	60.95 (2.18) <sup>e</sup>
MCH (pg)	20.35 (0.68)	19.95 (1.35)	20.20 (0.55)	20.00 (0.60)	19.25 (0.77)	19.10 (1.00)	18.95 (0.45)	19.60 (0.88)
MCHC (g/dL)	32.00 (0.78)	32.10 (0.33)	32.35 (0.72)	31.80 (0.50)	33.10 (0.90)	33.40 (0.40)	33.25 (0.35)	32.30 (0.30) <sup>d,e</sup>
RDW (%)	14.05 (1.53)	13.95 (1.15)	13.10 (1.13)	14.30 (1.20)	12.45 (0.25)	12.70 (0.80)	12.95 (0.40)	12.20 (0.57) <sup>e</sup>
HDW (g/dL)	2.27 (0.29)	2.30 (0.09)	2.20 (0.20)	2.44 (0.25) <sup>e</sup>	2.37 (0.19)	2.37 (0.16)	2.45 (0.16)	2.37 (0.32)
Reticulocytes, absolute (10 <sup>3</sup> /mm <sup>3</sup> )	378.30 (90.65)	359.65 (38.03)	314.20 (33.35) <sup>c</sup>	373.30 (106.50) <sup>e</sup>	277.80 (60.63)	256.70 (53.50)	277.25 (42.00)	325.95 (60.38) <sup>c,d</sup>
Platelets (10 <sup>3</sup> /mm <sup>3</sup> )	894.50 (93.00)	1,052.00 (145.00)	1,086.00 (192.25)	728.00 (86.00) <sup>c,d,e</sup>	822.00 (169.00)	801.00 (306.00)	939.00 (314.75)	603.50 (524.00) <sup>e</sup>
WBC (10 <sup>3</sup> /mm <sup>3</sup> )	7.95 (1.93)	8.40 (2.53)	10.05 (3.28)	13.70 (4.90) <sup>c,d</sup>	6.95 (2.43)	6.50 (3.50)	10.75 (3.68) <sup>c</sup>	8.15 (5.70)
Neutrophils, absolute (10 <sup>3</sup> /mm <sup>3</sup> )	1.48 (0.83)	2.04 (0.96)	1.85 (0.61)	8.40 (3.42) <sup>c,d,e</sup>	1.75 (0.77)	1.33 (0.99)	2.18 (1.30)	2.55 (2.72)
Lymphocytes, absolute (10 <sup>3</sup> /mm <sup>3</sup> )	5.49 (2.00)	6.03 (1.81)	6.69 (2.92)	4.24 (1.79) <sup>d,e</sup>	4.40 (1.75)	4.78 (3.21)	7.13 (1.76) <sup>c</sup>	5.56 (2.93)
Monocytes, absolute (10 <sup>3</sup> /mm <sup>3</sup> )	0.19 (0.16)	0.22 (0.20)	0.28 (0.10)	0.93 (0.29) <sup>c,d,e</sup>	0.17 (0.09)	0.17 (0.08)	0.39 (0.13) <sup>c,d</sup>	0.33 (0.26) <sup>c</sup>
Eosinophils, absolute (10 <sup>3</sup> /mm <sup>3</sup> )	0.27 (0.05)	0.37 (0.10)	0.31 (0.24)	0.15 (0.06) <sup>c,d,e</sup>	0.28 (0.22)	0.30 (0.23)	0.33 (0.14)	0.13 (0.06) <sup>c,e</sup>
Basophils, absolute (10 <sup>3</sup> /mm <sup>3</sup> )	0.02 (0.01)	0.03 (0.02)	0.03 (0.02)	0.03 (0.03)	0.02 (0.03)	0.02 (0.02)	0.04 (0.02)	0.06 (0.06)
LUC, absolute (10 <sup>3</sup> /mm <sup>3</sup> )	0.02 (0.01)	0.03 (0.02)	0.03 (0.02)	0.07 (0.05) <sup>c,d,e</sup>	0.02 (0.03)	0.02 (0.03)	0.04 (0.03)	0.05 (0.03)

<sup>a</sup>RBC, red blood cell count; MCV, mean cell volume; MCH, mean cell hemoglobin; MCHC, mean cell hemoglobin concentration; RDW, RBC volume distribution width; HDW, hemoglobin concentration distribution width; WBC, white blood cell count; LUC, large unclassified cells.

<sup>b</sup>Data are median (interquartile range [IQR]).

<sup>c</sup>P < 0.05 compared with control (0 mg/kg).

<sup>d</sup>P < 0.05 compared with 5 mg/kg.

<sup>e</sup>P < 0.05 compared with 10 mg/kg.

<sup>f</sup>Measurement on day of unscheduled euthanasia (day 2), excludes animals found dead.

**TABLE 5** Serum biochemical data for male and female rats at the end of treatment

Parameter <sup>a</sup>	Value <sup>b</sup> for rats at indicated dose							
	Male				Female			
	0 mg/kg	5 mg/kg	10 mg/kg	20 mg/kg <sup>f</sup>	0 mg/kg	5 mg/kg	10 mg/kg	20 mg/kg <sup>f</sup>
ALT (U/L)	42.5 (5.5)	40.0 (9.8)	32.5 (4.5)	74.0 (38.0) <sup>d,e</sup>	33.0 (8.0)	35.0 (7.0)	32.5 (6.0)	62.0 (28.5) <sup>c,d,e</sup>
AST (U/L)	158.5 (45.8)	133.0 (34.0)	113.5 (16.8)	245.0 (100.0) <sup>d,e</sup>	149.0 (22.0)	139.0 (35.0)	122.0 (14.3)	397.0 (345.5) <sup>d,e</sup>
ALP (U/L)	248.5 (72.8)	212.0 (40.3)	212.5 (51.5)	232.0 (45.0)	124.0 (28.0)	92.0 (21.0)	109.5 (30.5)	142.0 (34.5) <sup>d,e</sup>
Albumin (g/dL)	3.7 (0.2)	3.8 (0.0)	3.7 (0.2)	2.7 (0.0) <sup>c,d,e</sup>	3.6 (0.2)	3.9 (0.3)	3.9 (0.1)	3.0 (0.6) <sup>d,e</sup>
Globulin (g/dL)	1.6 (0.2)	1.7 (0.2)	1.6 (0.2)	1.0 (0.0) <sup>c,d,e</sup>	1.7 (0.1)	1.8 (0.1)	1.8 (0.2)	1.0 (0.3) <sup>c,d,e</sup>
A/G	2.4 (0.4)	2.2 (0.3)	2.4 (0.2)	2.7 (0.1) <sup>c,d,e</sup>	2.2 (0.1)	2.1 (0.2)	2.2 (0.2)	3.0 (0.4) <sup>c,d,e</sup>
GGT (U/L)	0.0 (0.0)	0.0 (0.0)	0.0 (0.0)	0.0 (0.0)	0.0 (0.0)	0.0 (0.0)	0.0 (0.0)	4.0 (5.5) <sup>c,d,e</sup>
T-Bil (mg/dL)	0.0 (0.0)	0.0 (0.0)	0.0 (0.0)	0.1 (0.2)	0.0 (0.0)	0.0 (0.0)	0.0 (0.0)	0.0 (0.0)
TP (g/dL)	5.2 (0.3)	5.5 (0.2)	5.4 (0.3)	3.7 (0.1) <sup>c,d,e</sup>	5.4 (0.4)	5.8 (0.5)	5.7 (0.4)	3.9 (0.8) <sup>c,d,e</sup>
Cholesterol (mg/dL)	59.5 (13.0)	70.5 (10.3)	66.0 (14.3)	67.0 (7.0)	52.0 (7.0)	55.0 (15.0)	55.0 (26.5)	52.0 (6.5)
Triglycerides (mg/dL)	29.0 (11.5)	37.0 (21.5)	29.0 (5.3)	193.0 (111.0) <sup>c,d,e</sup>	22.0 (4.0)	25.0 (7.0)	26.0 (11.5)	106.0 (36.5) <sup>c,d,e</sup>
Glucose (mg/dL)	87.0 (6.5)	72.5 (16.3)	83.0 (6.8)	175.0 (35.0) <sup>c,d,e</sup>	105.0 (7.0)	97.0 (16.0)	99.0 (5.5)	218.0 (70.0) <sup>c,d,e</sup>
Creatinine (mg/dL)	0.2 (0.0)	0.2 (0.1)	0.3 (0.1)	0.4 (0.1) <sup>c,d,e</sup>	0.3 (0.0)	0.3 (0.0)	0.3 (0.0)	0.5 (0.2) <sup>c,d,e</sup>
CK (U/L)	828.0 (341.5)	765.5 (395.5)	612.5 (254.8)	707.0 (615.0)	914.0 (450.0)	792.0 (198.0)	473.5 (211.3)	1,506.0 (2,604.5)
Urea N (mg/dL)	17.5 (4.3)	16.5 (4.0)	19.0 (3.5)	28.0 (6.0) <sup>c,d,e</sup>	20.0 (1.0)	20.0 (2.0)	21.0 (1.8)	20.0 (3.0)
Sodium (mmol/L)	144.5 (1.8)	144.0 (1.8)	144.0 (0.0)	140.0 (2.0) <sup>c,d,e</sup>	145.0 (3.0)	143.0 (1.0)	142.5 (1.0)	141.0 (2.5) <sup>f</sup>
Calcium (mg/dL)	9.6 (0.2)	9.8 (0.4)	9.7 (0.2)	9.4 (0.5) <sup>d</sup>	9.6 (0.2)	9.8 (0.2)	10.0 (0.3)	10.3 (0.6) <sup>c,d</sup>
Chloride (mmol/L)	105.0 (1.8)	104.5 (1.8)	105.0 (1.0)	101.0 (1.0) <sup>c,d,e</sup>	105.0 (3.0)	105.0 (2.0)	105.0 (2.0)	104.0 (3.0)
Phos (mg/dL)	8.3 (0.7)	8.5 (0.5)	8.6 (1.0)	9.3 (3.8)	7.6 (0.7)	7.3 (0.8)	7.1 (0.8)	9.3 (5.0)
Potassium (mmol/L)	4.8 (0.1)	5.2 (0.2)	5.1 (0.3)	5.1 (0.6)	4.4 (0.4)	4.9 (0.4)	5.1 (0.5)	4.9 (0.7)

<sup>a</sup>ALT, alanine aminotransferase; AST, aspartate aminotransferase; ALP, alkaline phosphatase; A/G, albumin/globulin ratio; GGT, gamma-glutamyltransferase; T-Bil, total bilirubin; TP, total protein; CK, creatine kinase; urea N, serum urea nitrogen; Phos, inorganic phosphorus.

<sup>b</sup>Data are median (IQR).

<sup>c</sup> $P < 0.05$  compared with control (0 mg/kg).

<sup>d</sup> $P < 0.05$  compared with 5 mg/kg.

<sup>e</sup> $P < 0.05$  compared with 10 mg/kg.

<sup>f</sup>Measurement on day of unscheduled euthanasia (day 2) excludes animals found dead.

(Table 5). At the end of recovery, glucose levels were slightly elevated in female rats at 10 mg/kg/day (data not shown). At the highest dose examined (20 mg/kg), chloride and albumin levels significantly decreased while serum urea nitrogen (urea N) levels increased in male rats on day 2 compared to controls. In female rats, alanine aminotransferase (ALT), calcium, and gamma-glutamyl transferase (GGT) levels were significantly elevated compared to controls. In both male and female rats, the albumin/globulin ratio (A/G) and creatinine, glucose, and triglyceride levels were significantly elevated while total protein (TP), sodium, and globulin levels were significantly reduced in comparison with controls. Albumin, A/G, globulin, urea N, TP, and triglyceride levels were outside the HCR in male rats and A/G ratio, GGT, globulin, glucose, TP, and triglycerides were outside the HCR in female rats. The remaining parameters were within the HCR.

There were no treatment-related changes in coagulation parameters in male and female rats in the 5- or 10-mg/kg/day group at the end of treatment (Table 6) or the end of recovery (data not shown). However, at 20 mg/kg, the prothrombin time (PT) and activated partial thromboplastin time (APTT) were significantly elevated in both male and female rats, while fibrinogen levels decreased in male rats compared to controls at the end of treatment. Of these, fibrinogen levels were outside the HCR in male rats, and both PT and APTT were outside the HCR in female rats.

There were no treatment-related changes in urinalysis parameters for male and female rats receiving 5 or 10 mg/kg/day (data not shown). Due to early removal, overnight urine samples were not collected from rats in the 20-mg/kg group and therefore could not be assessed. No treatment-related abnormalities were detected during the postexposure ophthalmology assessments for any dosing group. In this study, treatment-related effects on the injection site could not be assessed due to surgical catheterization. A summary of the main histopathological findings in the adrenal glands, liver, and lungs at the end of treatment are described in Table S3. Specifically, histopathological evaluations of rats in the 20-mg/kg group showed discolorations in the

**TABLE 6** Coagulation data for male and female rats and cynomolgus monkeys at the end of treatment<sup>a</sup>

Group and dose	PT (s)	APTT (s)	Fibrinogen (mg/dL)
Rats			
Male			
0 mg/kg	16.25 (1.60)	14.05 (2.85)	263.50 (49.75)
5 mg/kg	15.95 (0.50)	14.80 (0.98)	262.50 (9.00)
10 mg/kg	17.50 (1.40)	14.60 (1.05)	261.00 (54.75)
20 mg/kg <sup>e</sup>	21.25 (1.40) <sup>b,c</sup>	18.50 (3.13) <sup>b,c,d</sup>	98.00 (18.50) <sup>b,c,d</sup>
Female			
0 mg/kg	16.30 (0.70)	10.50 (1.90)	269.00 (68.00)
5 mg/kg	16.30 (1.40)	10.60 (0.70)	223.00 (80.00)
10 mg/kg	17.05 (0.60)	10.85 (2.43)	283.00 (36.50)
20 mg/kg <sup>e</sup>	23.45 (9.75) <sup>b,c</sup>	29.20 (20.65) <sup>b,c,d</sup>	83.00 (151.75) <sup>d</sup>
Cynomolgus monkeys			
Male			
0 mg/kg	12.20 (0.80)	22.00 (1.90)	228.00 (22.00)
5 mg/kg	12.00 (0.55)	21.60 (0.80)	306.00 (49.50)
10 mg/kg	12.00 (0.25)	21.10 (0.45)	285.00 (22.50)
15 mg/kg	12.25 (0.83)	22.10 (1.65)	336.00 (114.00)
Female			
0 mg/kg	12.50 (0.80)	22.00 (0.30)	173.00 (75.00)
5 mg/kg	12.20 (0.25)	22.40 (2.05)	238.00 (40.50)
10 mg/kg	11.80 (0.25)	20.80 (0.55)	294.00 (7.50)
15 mg/kg	12.30 (0.50)	22.60 (0.90)	300.00 (57.00) <sup>d</sup>

<sup>a</sup>PT, prothrombin time; APTT activated partial thromboplastin time. Data are median (IQR).

<sup>b</sup> $P < 0.05$  compared with control (0 mg/kg).

<sup>c</sup> $P < 0.05$  compared with 5 mg/kg.

<sup>d</sup> $P < 0.05$  compared with 10 mg.

<sup>e</sup>Measurement on day of unscheduled euthanasia (day 2) excludes animals found dead.

kidney, brain, and lungs, with bronchi and trachea filled with fluids at interim euthanasia. There were no macroscopic findings related to RTD-1 treatment in any dose groups at interim euthanasia (for 20-mg/kg group, day 2), terminal euthanasia (day 8), or recovery euthanasia (day 24). Key treatment-related microscopic findings at the end of treatment included dose-dependent increased incidence of minimal to mild liver necrosis in female rats administered 5 and 10 mg/kg/day. However, liver necrosis was not present in female animals (5 and 10 mg/kg/day) euthanized at the end of the recovery period and did not lead to increases in parameters included in the liver function panels (TP, albumin, total bilirubin, and liver enzymes). Adverse treatment-related severity ranging from minimal to moderate liver necrosis, defined by focal to multifocal areas of lytic to coagulative necrosis, was observed in male rats administered 20 mg/kg. Mild to severe adrenal necrosis, characterized by unilateral to bilateral coagulative cortical to corticomedullary necrosis, was observed in both male and female rats administered 20 mg/kg.

Based on the lack of adverse clinical signs or abnormalities in parameters at the 10-mg/kg/day dose, the no observed adverse effect level (NOAEL) was established at 10 mg/kg/day in rats. The lowest observed adverse effect level (LOAEL), which the FDA defines as the lowest dose tested in preclinical species with adverse effects, was established at 20 mg/kg in rats (19).

**(ii) Cynomolgus monkeys.** Overall, RTD-1 at doses up to 15 mg/kg/day was well tolerated in male and female monkeys. In the non-GLP dose range-finding study, all animals survived the study without any treatment-related adverse clinical signs. The maximum tolerated dose (MTD) was established at 15 mg/kg/day based on these data. Similarly, in the GLP-compliant 10-day repeat-dose TK study, no mortality or unscheduled euthanasia occurred at any dose level. In addition, no significant changes in body weight were observed in the monkeys. Treatment-related decrease in food consumption was observed in females at 10 mg/kg/day and in both sexes at 15 mg/kg/day

during the dosing phase; however, the animals recovered to baseline by the end of recovery, and the changes in food consumption did not translate to changes in body weight or adverse clinical observations.

Treatment-related hematological changes at the end of treatment included statistically significant but modest increases in absolute LUC counts in male monkeys and absolute monocytes in female monkeys at 15 mg/kg/day compared to the respective controls (Table 7). However, the increase in absolute LUC counts resolved by the end of recovery (data not shown) and the elevated absolute monocyte counts observed in female monkeys were within the HCR for female cynomolgus monkeys (20). The histopathological examinations of bone marrow samples from sternum and femur samples were within normal limits. Most notable, treatment-related changes in serum biochemical parameters included a slight reduction in inorganic phosphorus (Phos) level and an elevated glucose level in female monkeys at 15 mg/kg/day at the end of treatment (Table 8). However, these changes were small in magnitude and remained within the HCR for female cynomolgus monkeys. A trend toward an increase in fibrinogen levels was noted in all treated monkeys at the end of treatment compared to the control group and baseline levels (Table 6), but the changes did not reach statistical significance and returned to baseline by the end of the recovery period (data not shown). There were no treatment-related changes in urinalysis parameters or abnormalities in postexposure ophthalmologic assessments or the electrocardiogram from cynomolgus monkeys at any dose level (data not shown). A summary of the main histopathological findings in the adrenal glands, liver, and lungs at the end of treatment are described in Table S4. There were no major histological findings at the end of the recovery period (data not shown). The lack of significant alterations in clinical pathology parameters in any of the animals with doses up to 15 mg/kg/day corroborates the results from the non-GLP dose range study in cynomolgus monkeys, which also established an MTD of 15 mg/kg/day based on no adverse effects on mortality, clinical observations, or body weight with up to 15 mg/kg/day i.v. RTD-1 treatment. Due to the small number of measurements taken at the end of the recovery period, statistical analyses of the clinical pathology parameters at this time point could not be performed.

Procedure-related gross observations were recorded at the injection sites of three animals at 15 mg/kg/day, which included abrasions and abnormal texture likely due to repeat catheterization. However, there were no macroscopic findings related to treatment at the end of treatment or recovery. In the main group, microscopic evaluations revealed treatment-related thrombosis at the injection sites at the end of treatment, although there was a lack of a dose trend in incidence and/or severity. In the recovery group, treatment-related thrombosis at the injection site, acute inflammation, edema, hemorrhage, and fibrosis were present in animals receiving 15 mg/kg/day at the end of recovery. However, comparable observations were also present at the injection sites of control animals in the recovery group, which include minimal to mild injection site fibrosis and mild chronic thrombosis, suggesting that these findings are procedure related. Lastly, minimal to mild intravascular thrombosis (thromboembolism) was observed in the lungs of only the treated animals (males administered  $\geq 10$  mg/kg/day and females administered  $\geq 5$  mg/kg/day) at the end of treatment (day 11). The thrombi within the lungs contained differing numbers of inflammatory cells both within the thrombi and in the surrounding connective tissues, and thrombi in the lungs were present predominately in midsize to small arteries and capillaries in the alveolar walls. Thromboembolism was concluded to be related to the peptide administration due to the composition of the thrombi found in the lung, which were likely embolic from the thrombi formed at the injection site. These findings were also resolved by the end of the recovery period, as thrombosis was not identified in any lung sections in the control group or monkeys administered 15 mg/kg/day.

Given that the repeat administration of RTD-1 of up to 15 mg/kg/day was well tolerated in both sexes, NOAEL was established at 15 mg/kg/day in cynomolgus monkeys. The LOAEL could not be determined in cynomolgus monkeys, as the highest dose

**TABLE 7** Hematological results for male and female cynomolgus monkeys at the end of treatment

Parameter <sup>a</sup>	Value <sup>b</sup> for monkeys at indicated dose							
	Male			Female				
	0 mg/kg	5 mg/kg	10 mg/kg	15 mg/kg	0 mg/kg	5 mg/kg	10 mg/kg	15 mg/kg
RBC (10 <sup>6</sup> /mm <sup>3</sup> )	5.92 (0.35)	6.06 (0.42)	6.35 (0.58)	5.56 (0.40)	6.27 (0.58)	6.05 (0.47)	5.30 (0.94)	6.04 (1.28)
Hemoglobin (g/dL)	12.40 (0.60)	12.70 (0.85)	11.90 (1.30)	11.10 (0.90)	12.50 (0.10)	12.90 (0.35)	10.70 (1.25)	10.90 (1.70)
Hematocrit (%)	42.40 (2.30)	43.10 (3.05)	42.60 (5.20)	38.40 (2.30)	42.20 (3.50)	43.80 (3.15)	38.50 (4.60)	38.50 (6.90)
MCV (fL)	71.80 (0.70)	75.10 (2.10)	72.00 (4.00)	71.20 (3.40)	70.60 (2.90)	69.20 (1.70)	69.70 (4.30)	68.90 (2.00)
MCH (pg)	21.00 (0.40)	19.80 (0.55)	20.30 (1.00)	20.20 (0.90)	21.40 (2.20)	21.20 (1.10)	20.20 (1.00)	19.90 (0.30)
MCHC (g/dL)	29.40 (0.90)	26.40 (1.55)	27.90 (0.35)	28.90 (1.20)	30.80 (2.60)	29.50 (1.35)	28.80 (0.70)	28.80 (1.10)
RDW (%)	15.10 (0.50)	15.40 (1.00)	17.20 (1.35)	14.80 (0.80)	16.10 (1.70)	15.10 (0.50)	15.10 (0.70)	14.70 (1.80)
Reticulocytes, absolute (10 <sup>9</sup> /L)	71.80 (38.10)	43.70 (23.20)	60.00 (71.70)	69.10 (47.50)	52.80 (19.30)	53.60 (17.00)	70.30 (33.40)	83.90 (46.10)
Platelets (10 <sup>3</sup> /mm <sup>3</sup> )	386.00 (70.25)	358.00 (21.50)	450.00 (114.00)	634.00 (42.00) <sup>d</sup>	358.00 (54.00)	576.00 (58.00)	497.00 (214.50)	513.00 (299.00)
WBC (10 <sup>3</sup> /mm <sup>3</sup> )	8.70 (4.80)	14.70 (5.95)	11.00 (1.75)	14.90 (12.80)	11.20 (1.70)	12.70 (2.30)	10.70 (6.80)	16.10 (5.40)
Neutrophils, absolute (10 <sup>3</sup> /mm <sup>3</sup> )	2.70 (1.33)	4.65 (3.33)	4.31 (1.38)	7.62 (9.59)	4.99 (3.24)	6.43 (2.10)	5.08 (5.64)	11.31 (5.67)
Lymphocytes, absolute (10 <sup>3</sup> /mm <sup>3</sup> )	4.82 (1.22)	6.85 (3.12)	5.85 (2.85)	4.78 (2.17)	4.98 (3.17)	3.40 (1.18)	4.46 (1.00)	5.09 (2.32)
Monocytes, absolute (10 <sup>3</sup> /mm <sup>3</sup> )	0.42 (0.38)	0.74 (0.23)	0.63 (0.18)	1.10 (0.74)	0.51 (0.06)	0.53 (0.21)	0.66 (0.13)	0.79 (0.15) <sup>c</sup>
Eosinophils, absolute (10 <sup>3</sup> /mm <sup>3</sup> )	0.09 (0.16)	0.26 (0.12)	0.20 (0.06)	0.39 (0.70)	0.18 (0.08)	0.32 (0.27)	0.40 (0.06)	0.34 (0.10)
Basophils, absolute (10 <sup>3</sup> /mm <sup>3</sup> )	0.05 (0.02)	0.12 (0.08)	0.08 (0.04)	0.11 (0.10)	0.09 (0.02)	0.05 (0.01)	0.06 (0.04)	0.12 (0.01)
LUC, absolute (10 <sup>3</sup> /mm <sup>3</sup> )	0.08 (0.02)	0.15 (0.07)	0.15 (0.01)	0.17 (0.11) <sup>c</sup>	0.12 (0.07)	0.11 (0.02)	0.10 (0.01)	0.16 (0.06)

<sup>a</sup>RBC, red blood cell count; MCV, mean cell volume; RDW, RBC volume distribution width; MCHC, mean cell hemoglobin concentration; MCH, mean cell hemoglobin; WBC, white blood cell count; LUC, large unclassified cells.  
<sup>b</sup>Data are median (IQR).

<sup>c</sup>P < 0.05 compared with control (0 mg/kg).

<sup>d</sup>P < 0.05 compared with 5 mg/kg.

**TABLE 8** Serum biochemical data for male and female cynomolgus monkeys at the end of treatment

Parameter <sup>a</sup>	Value <sup>b</sup> for monkeys at indicated dose							
	Male				Female			
	Control	5 mg/kg	10 mg/kg	15 mg/kg	Control	5 mg/kg	10 mg/kg	15 mg/kg
ALT (U/L)	63.0 (13.0)	172.0 (125.0)	105.0 (26.5)	88.0 (17.0)	584.0 (124.0)	112.0 (50.0)	126.0 (87.5)	92.0 (36.0)
AST (U/L)	60.0 (31.0)	122.0 (190.0)	105.0 (43.5)	103.0 (40.0)	142.0 (37.0)	69.0 (22.0)	104.0 (16.0)	95.0 (45.0)
ALP (U/L)	664.0 (120.0)	802.0 (253.0)	753.0 (3.5)	957.0 (638.0)	682.0 (117.0)	576.0 (132.0)	915.0 (64.0)	943.0 (411.0)
Albumin (g/dL)	4.6 (0.1)	4.8 (0.2)	4.7 (0.2)	4.4 (0.2)	4.4 (0.1)	4.5 (0.5)	4.3 (0.1)	4.3 (0.6)
Globulin (g/dL)	2.5 (0.0)	2.7 (0.1)	2.9 (0.4)	2.9 (0.5)	2.5 (0.1)	2.7 (0.4)	2.7 (0.4)	2.8 (0.1)
A/G	1.8 (0.1)	1.8 (0.1)	1.7 (0.2)	1.6 (0.2)	1.7 (0.1)	1.7 (0.2)	1.6 (0.2)	1.5 (0.0)
GGT (U/L)	125.0 (4.0)	137.0 (31.5)	119.0 (32.5)	101.0 (6.0)	128.0 (37.0)	92.0 (14.0)	88.0 (7.0)	99.0 (37.0)
T-Bil (mg/dL)	0.3 (0.1)	0.3 (0.1)	0.3 (0.0)	0.2 (0.2)	0.3 (0.2)	0.2 (0.0)	0.2 (0.1)	0.2 (0.2)
TP (g/dL)	7.1 (0.1)	7.5 (0.2)	7.5 (0.5)	7.5 (0.8)	6.9 (0.2)	7.6 (0.7)	7.0 (0.3)	7.1 (0.8)
Cholesterol (mg/dL)	88.0 (14.0)	110.0 (15.5)	99.0 (16.5)	105.0 (50.0)	133.0 (24.0)	104.0 (17.5)	91.0 (10.5)	94.0 (13.0)
Triglycerides (mg/dL)	33.0 (4.0)	46.0 (18.5)	32.0 (6.0)	78.0 (52.0)	33.0 (5.0)	49.0 (8.5)	49.0 (1.5)	56.0 (11.0)
Glucose (mg/dL)	66.0 (7.0)	111.0 (26.5)	71.0 (23.0)	67.0 (5.0)	54.0 (2.0)	60.0 (7.5)	59.0 (6.5)	78.0 (18.0) <sup>c</sup>
Creatinine (mg/dL)	0.6 (0.1)	0.8 (0.2)	0.6 (0.1)	0.6 (0.1)	0.5 (0.1)	0.5 (0.1)	0.6 (0.1)	0.7 (0.1)
CK (U/L)	215.0 (1,159.0)	888.0 (13,478.0)	515.0 (2,756.5)	518.0 (1,392.0)	405.0 (288.0)	301.0 (38.0)	1,102.0 (1,584.0)	891.0 (603.0)
Urea N (mg/dL)	13.0 (2.0)	15.0 (3.5)	20.0 (3.5)	15.0 (2.0)	15.0 (2.0)	15.0 (4.0)	16.0 (4.5)	18.0 (1.0)
Sodium (mmol/L)	148.0 (3.0)	147.0 (4.0)	150.0 (3.0)	149.0 (2.0)	148.0 (2.0)	146.0 (0.0)	146.0 (3.0)	146.0 (4.0)
Calcium (mg/dL)	10.0 (0.1)	9.8 (0.5)	10.5 (0.4)	10.1 (0.3)	9.8 (0.5)	10.0 (0.4)	10.0 (0.1)	10.2 (0.4)
Chloride (mmol/L)	110.0 (2.0)	110.0 (2.0)	110.0 (1.5)	112.0 (1.0)	110.0 (4.0)	107.0 (1.5)	109.0 (2.0)	111.0 (1.0)
Phos (mg/dL)	6.5 (0.5)	5.5 (1.7)	5.4 (0.8)	5.2 (0.6)	6.1 (0.2)	5.7 (0.2)	5.3 (0.6)	5.3 (0.3) <sup>c</sup>
Potassium (mmol/L)	5.5 (0.7)	6.0 (1.4)	5.9 (0.9)	5.8 (0.6)	5.1 (0.1)	4.9 (0.6)	5.1 (0.9)	6.0 (1.0)

<sup>a</sup>ALT, alanine aminotransferase; AST, aspartate aminotransferase; ALP, alkaline phosphatase; A/G, albumin/globulin ratio; GGT, gamma-glutamyltransferase; T-Bil, total bilirubin; TP, total protein; CK, creatine kinase; urea N, serum urea nitrogen; Phos, inorganic phosphorus.

<sup>b</sup>Data are median (IQR).

<sup>c</sup>*P* < 0.05 compared with control (0 mg/kg).

examined in the GLP study was well tolerated. Based on this analysis, the HEDs that are equivalent to the NOAEL and LOAEL in rats are 3.2 mg/kg/day and 11.8 mg/kg/day, respectively, for a 70-kg individual, and the HED that is equivalent to the NOAEL in cynomolgus monkeys is 16.1 mg/kg/day for a 70-kg individual.

## DISCUSSION

Despite the recent development of COVID-19 vaccines, the emergence of new COVID-19 variants remains a major threat to global health. Dysregulated inflammatory response is one of the key characteristics observed in severe COVID-19 patients and is the main factor contributing to multiple organ failure and mortality (21, 22). Based on the results of the RECOVERY trial, the use of corticosteroids has shown to be effective in reducing mortality in severely ill COVID-19 patients receiving supplemental oxygen, which highlights the importance of targeting the systemic inflammation caused by COVID-19 to improve patient outcomes (8). However, at present, there are a limited number of safe and effective treatments available for COVID-19 pneumonia. In the current analysis, the PK and safety of i.v. RTD-1 were examined in various preclinical studies in preparation for planned clinical trials of RTD-1 for the treatment of COVID-19 pneumonia.

Single and multiple-ascending-dose studies performed in rats and cynomolgus monkeys demonstrated the excellent safety profile of i.v. RTD-1 administration. Repeat administration of RTD-1 was well tolerated in rats at doses up to 10 mg/kg/day, and therefore, the NOAEL in rats was established at 10 mg/kg/day. Treatment-related mortality and adverse clinical signs were observed in rats treated at 20 mg/kg, including cold to touch, abnormal body color, inability to walk, extreme dehydration, and tremors. In cynomolgus monkeys, single and repeated daily dose administration of RTD-1 was tolerated up to 15 mg/kg/day, with no major treatment-related adverse findings or toxicities. Given the lack of adverse findings, the NOAEL was established at 15 mg/kg/day in cynomolgus monkeys. The NOAEL in the cynomolgus monkeys was established at a higher dose than that in the rats, demonstrating that RTD-1 was better tolerated in cynomolgus monkeys. Most changes noted in hematological, serum chemistry, and coagulation

parameters in both rats and cynomolgus monkeys were of low magnitude, lacked consistency between the two species, lacked a dose dependence, and/or were reversible by the end of the recovery period. Therefore, these data demonstrate the safety of i.v. RTD-1 at a dose up to 10 mg/kg/day in rats and 15 mg/kg/day in cynomolgus monkeys.

The PK of intravenous RTD-1 following single and multiple ascending doses in multiple species is characterized by extensive tissue distribution and prolonged elimination. The  $V_{ss}$  normalized to the body weight of the animals receiving 5 mg/kg of RTD-1 varied across species, with 1,048, 1,461, and 550 mL/kg in mice, rats, and cynomolgus monkeys, respectively. The relatively large  $V_{ss}$  indicates that RTD-1 distributes extensively to tissues. The biodistribution study confirmed extensive tissue distribution, particularly in the liver. Relevant to the treatment of COVID-19, RTD-1 distribution to the lungs was less than that to the plasma; however, it remained measurable at 24 h following a single dose administration and exceeded values for most other tissues. The prolonged elimination half-life observed in cynomolgus monkeys in the recovery group (47.2 h) is suggestive of tissue redistribution. Future studies involving whole-body tissue PK analysis to evaluate the time course of drug disposition more extensively within tissues are planned.

Analysis of the single and multiple-ascending-dose studies in rats and monkeys showed a greater-than-dose-proportional increase in  $AUC_{0-\infty}$  and  $C_{max}$  suggestive of nonlinear PK. Several therapeutic proteins exhibit nonlinear PK mediated by different mechanisms. For instance, exenatide and recombinant human interferon (IFN) (e.g., IFN- $\beta$ 1a) display nonlinear kinetics due to the saturation of the elimination pathway, such as target-mediated drug disposition (TMDD) (23, 24). Alternatively, nonlinear PK of cyclosporine and erythropoietin were attributable to the saturation of tissue binding and receptors in target tissues, respectively (25, 26). The widespread distribution of [ $^{14}$ C]RTD-1 in rats in the biodistribution study, which could explain the large  $V_{ss}$  estimated in the preclinical PK studies, suggests that saturation of the peptide within these tissues may be one potential source of nonlinearity. Since the greatest accumulation of RTD-1 occurred in the liver and kidney, a dose-dependent decrease in CL observed in rats and cynomolgus monkeys could also explain the nonlinearity. Consistent with data from other small peptides (<10 kDa) which are predominately cleared through the glomerular filtration, appreciable amounts of [ $^{14}$ C]RTD-1 were recovered from the urine (accounting for 7% at 24 h). In addition, a relatively significant portion was recovered in feces (accounting for 4% at 24 h), indicating that elimination of RTD-1 occurs through renal and biliary excretion (27, 28). Therefore, the nonlinear PK of RTD-1 may be attributable to saturation of uptake and/or efflux transporters present in the liver or kidney. However, the definitive role of hepatic/renal transporters in the distribution and elimination of RTD-1 requires further investigation.

Interspecies allometric scaling is a valuable tool that enables the extrapolation of PK data from preclinical species to humans and is commonly used to predict an appropriate dosage for FIH clinical trials. Since RTD-1 is believed to follow linear PK at the HED for efficacy, as evidenced by dose-proportional increases in the  $AUC_{0-\infty}$  at lower doses in cynomolgus monkeys (0.3 to 3 mg/kg), we performed interspecies allometric scaling using simple allometry to predict human PK. For macromolecules that are renally excreted, human CL can be adequately predicted using the simple allometric equation (29). As three or more preclinical species are typically needed to reliably scale the parameters to humans, available single-dose data from mice and vervet were included in the analysis (30). The estimated allometric scaling exponents of 0.8302 and 0.8651 for CL and  $V_{ss}$ , respectively, agree with the values reported for other therapeutic proteins, which are 0.65 to 0.84 for CL and 0.84 to 1.02 for  $V_{ss}$  (31).

The target  $AUC_{0-\infty}$  was previously established in a mouse model of lipopolysaccharide (LPS)-induced ALI, where a single subcutaneous injection of 5 or 25 mg/kg RTD-1 resulted in mean  $AUC_{0-\infty}$  values of 3,869 and 9,001 ng · h/mL, respectively. RTD-1 treatment at both doses led to attenuation of the airway inflammatory response through inhibition of proinflammatory cytokine production, peroxidase activity, and neutrophil

recruitment and protected against lung injury (3). RTD-1 treatment (25 mg/kg) administered 0 h after LPS instillation was associated with approximately 66%, 63%, and 80% decreases in IL-6, IP-10 (CXCL10), and IFN- $\gamma$ , respectively, in bronchoalveolar lavage fluid, whereas dexamethasone treatment (2 mg/kg) led to approximately 26%, 50%, and 43% decreases in IL-6, IP-10 (CXCL10), and IFN- $\gamma$ , respectively (3).

The HED of 0.36 mg/kg daily was determined using the predicted human CL (6.48 L/h) from interspecies allometric scaling and the target  $AUC_{0-\infty}$  for efficacy (from the murine model of endotoxin-induced ALI). Based on the FDA's recommendation for a 10-fold safety factor, the predicted FIH dose in a clinical trial is approximately 0.036 mg/kg for an adult (32, 33). This approximation of the dose for the FIH study is predicted to be well below the NOAEL established by preclinical animals and therefore projected to be safe in humans. The HED equivalent to the NOAEL in cynomolgus monkeys of 16.1 mg/kg was higher than both the HED equivalents to the NOAEL and the LOAEL in rats (3.2 and 11.8 mg/kg, respectively). Since cynomolgus monkeys are more physiologically similar to humans than rats, doses up to 16.1 mg/kg may be tolerated in humans. Furthermore, this indicates that the HED required for efficacy (0.36 to 0.83 mg/kg) is approximately 19- to 45-fold lower than the HED calculated based on the NOAEL in cynomolgus monkeys, further ensuring safety in humans.

There were a few limitations to our analysis. First, simple allometry does not account for dose-dependent (nonlinear) processes and therefore may not be suitable for scaling the parameters to humans. However, since nonlinearity was more evident at higher dose ranges, we believe that at the doses selected for an FIH clinical trial, RTD-1 is predicted to exhibit linear PK. Second, the target  $AUC_{0-\infty}$  used to determine the FIH dose was established in a murine model of LPS-induced ALI and therefore may not reflect the actual target  $AUC_{0-\infty}$  required for efficacy in COVID-19 in humans. We believe this is an appropriate animal model to derive the target  $AUC_{0-\infty}$  for efficacy, as COVID-19-related pneumonia is characterized by excessive infiltration of neutrophils and overproduction of proinflammatory cytokines in the airway (34, 35).

In summary, we assessed the PK and safety of intravenous RTD-1 in mice, rats, cynomolgus monkeys, and a vervet and predicted the human PK using a simple allometric equation. Single-dose and multiple-ascending-dose studies in cynomolgus monkeys revealed a dose-dependent decrease in CL. The biodistribution of [ $^{14}\text{C}$ ]RTD-1 revealed that RTD-1 distributes extensively to tissues and, in particular, the liver. Recoverable  $^{14}\text{C}$  counts in the urine and feces indicate that renal and biliary excretion are the major routes of elimination. Further studies are warranted to investigate the kinetics of tissue distribution/elimination to identify the sources of nonlinearity. Lastly, repeat administrations of intravenous RTD-1 were well tolerated in rats and cynomolgus monkeys up to 10 mg/kg/day and 15 mg/kg/day, respectively, without any evidence of toxicity. The HED required to provide efficacy is well below the HED established based on the NOAEL in the cynomolgus monkey. Therefore, these results support the clinical investigation of RTD-1 for the treatment of COVID-19. The PK and safety of intravenous RTD-1 are being evaluated in a phase I/II clinical trial with patients hospitalized with COVID-19-related pneumonia (ClinicalTrials.gov identifier NCT04708236).

## MATERIALS AND METHODS

The pharmacokinetics and safety of i.v. RTD-1 were studied in mice, rats, cynomolgus monkeys, and a vervet. Lyophilized RTD-1 (purity > 98%) was dissolved in filter-sterilized saline solution and used for injections of mice and one vervet. RTD-1 solutions employing rats and cynomolgus monkeys were prepared by dilution of formulated RTD-1 (12.5 mg/mL in 1% propylene glycol, 20 mM sodium acetate, pH 6.5) in filter-sterilized saline. The summary of study design and schedule of safety assessments are given in Tables S1 and S2, respectively, in the supplemental material. The studies included single- and multiple-dose-ranging experiments. All protocols received local IACUC approval before the initiation of the studies.

**Pharmacokinetics. (i) Mice.** The murine pharmacokinetic study has been described previously (12). All procedures and protocols involving the use of animals were reviewed and approved by the University of Southern California (USC) IACUC (protocol no. 20538). Briefly, male (31.7 to 37.7 g) and female (25.2 to 35.6 g) CD-1 mice (Charles River Laboratories) were administered a single 5-mg/kg i.v. bolus injection of RTD-1 into the lateral tail vein. A total of 24 mice were separated into six groups

( $n = 2/\text{sex}/\text{group}$ ), with each group assigned to a single, predetermined time point. EDTA-anticoagulated blood samples were collected at 0.25, 1, 2, 4, 8, and 24 h postdose via terminal cardiac puncture. The collected samples were centrifuged to separate the plasma and stored at  $-80^{\circ}\text{C}$  until analysis.

**(ii) Rats.** Pharmacokinetics of RTD-1 in Sprague-Dawley rats was evaluated as part of a Good Laboratory Practice (GLP) 7-day toxicity study performed at Charles River Laboratories (Stilwell, Kansas). The study protocol was reviewed and approved by the Citoxlab USA IACUC and was conducted in accordance with guidelines from the USA National Research Council. On the day of the dosing (day 1), male (229 to 272 g) and female (186 to 214 g) rats ( $n = 6/\text{sex}/\text{group}$ ) were assigned to receive repeated doses of 0 (placebo), 5, 10, or 20 mg/kg/day of RTD-1 once daily for 7 days via i.v. infusion (20 min  $\pm$  3 min). The intravenous route was selected, as this is the intended route of administration for the treatment of COVID-19 pneumonia. The doses were chosen based on a pilot single-dose escalation study in rats, which established the MTD of 20 mg/kg (data not shown). Two subgroups of rats with alternating blood sampling schemes ( $n = 3/\text{sex}/\text{group}$ ) were assigned as follows: subgroup A with blood collections at 0 (predose), 0.5, 6, and 24 h postinfusion and subgroup B with blood collections at 0.083, 2, and 12 h postinfusion. The 24-h postinfusion samples on day 1 were taken before the administration of the dose on day 2. Serial blood samples were collected into  $\text{K}_2\text{EDTA}$  tubes at the above-mentioned time points on days 1 and 7 and once on day 25 (recovery). The samples were centrifuged at  $2,700 \times g$  for 10 min at  $5^{\circ}\text{C}$  to separate plasma from the blood and stored at  $-80^{\circ}\text{C}$  until analysis.

**(iii) Cynomolgus monkeys.** A non-GLP dose-range-finding PK study and a GLP 10-day toxicity study were conducted in cynomolgus monkeys (*Macaca fascicularis*) at Charles River Laboratories (Stilwell, Kansas). The study protocol was reviewed and approved by the Citoxlab USA IACUC and was conducted in accordance with guidelines from the USA National Research Council. The non-GLP dose-range-finding study included evaluation of a single ascending dose and a multiple dose. In the single-ascending-dose PK study, male (3.49 to 3.57 kg) and female (2.66 to 2.79 kg) cynomolgus monkeys ( $n = 1/\text{sex}/\text{group}$ ) were randomly assigned to one of two dose groups. Group 1 received a single dose of 0.3 mg/kg RTD-1 as an i.v. infusion (60 min  $\pm$  5 min) on day 1 and a single dose of 3 mg/kg RTD-1 on day 3, while group 2 received a single dose of 1 mg/kg RTD-1 on day 1 and a single dose of 10 mg/kg RTD-1 on day 3. The doses used in this study are based on a pilot study in cynomolgus monkeys which demonstrated the safety of single i.v. doses up to and including 10 mg/kg (data not shown). Blood samples were collected into  $\text{K}_2\text{EDTA}$  tubes at the following time points: predose and approximately 0.083, 0.25, 0.5, 1, 2, 4, 8, 12, and 24 h post-end of infusion, on days 1 and 3. In the multiple-dose study, repeated doses of 15 mg/kg RTD-1 were administered once daily for 7 days via i.v. infusion (60 min  $\pm$  5 min) ( $n = 1$  per sex). Serial blood samples were collected into  $\text{K}_2\text{EDTA}$  at predose and at approximately 0.083, 0.25, 0.5, 1, 2, 4, 8, 12, and 24 h post-end of infusion, on days 1, 4, and 7. The 24-h postinfusion samples on days 1 and 4 were taken before the administration of the dose on days 2 and 5, respectively. In the GLP 10-day toxicity study, PK was evaluated following multiple ascending doses of RTD-1. Male (2.52 to 3.65 kg) and female (2.39 to 3.18 kg) cynomolgus monkeys ( $n = 3\text{-}5/\text{sex}/\text{group}$ ) received repeated doses of 0 (placebo), 5, 10, or 15 mg/kg of RTD-1 once daily for 10 days via i.v. infusion (60 min  $\pm$  5 min). Serial blood samples were collected into  $\text{K}_2\text{EDTA}$  tubes at the following time points: predose and 0.083, 0.5, 2, 6, and 12 h postinfusion on day 1 and predose and 0.083, 0.5, 2, 6, 12, and 24 h postinfusion on day 10. Additional blood samples were collected on days 12 and 24 from monkeys that received 0 or 15 mg/kg ( $n = 2/\text{sex}/\text{group}$ ). All samples were centrifuged at  $\sim 2,700 \times g$  for 10 min at  $\sim 5^{\circ}\text{C}$  to isolate plasma and stored at  $-80^{\circ}\text{C}$  until analysis.

**(iv) Vervet.** As a pilot safety study, a single dose of RTD-1 at 3 mg/kg was administered to an adult male vervet/African green monkey (*Chlorocebus aethiops sabaues*) via i.v. bolus. Serial blood samples were collected at 0.5, 1, 4, 8, 24, 48, 72, 96, 120, and 192 h postadministration.

**Bioanalytical analysis.** Clarified plasma samples from mice were directly diluted into 5% formic acid-5% acetonitrile. Quantitative analysis of RTD-1 was performed by liquid chromatography-tandem mass spectrometry (LC-MS/MS) with reverse-phase liquid chromatography (XBridge BEH phenyl column;  $3.5 \mu\text{m}$ , 3 by 100 mm; Waters no. 186003328) on an Acquity H-class ultraperformance LC (UPLC) (Waters) coupled to a Xevo TQ-S tandem electrospray mass spectrometry running MassLynx V4.1 (Waters). Quantitative mass spectrometry was performed by multiple-reaction monitoring with the area under the curve determined by TargetLynx (Waters). A synthetic theta defensin-like peptide was used as an internal standard (IS). The lower limit of quantification (LLOQ) of the assay was 1 ng/mL. Intra- and interassay precision (percent coefficient of variation [CV]) was  $\leq 3\%$ , and intra- and interassay accuracy (% relative error) was  $\leq 5\%$ . Plasma RTD-1 concentration analyses for rats and cynomolgus monkey studies were performed at MicroConstants (San Diego, CA) by LC-MS/MS using a validated method with an LLOQ of 10.0 ng/mL. Details of the method are summarized in MicroConstants method no. MN20038. Clarified plasma samples from a serially sampled vervet were quantified using a Waters Acquity H-class UPLC. The plasma samples were diluted directly (1:10) into 5% formic acid-5% acetonitrile and quantified by photodiode array (PDA; AUC of 210 nm) by using a  $\text{C}_{18}$  XBridge BEH column ( $2.5 \mu\text{m}$ , 2.1 by 150 mm; Waters no. 186006709) and running Empower 3 software (Waters). RTD-1 peak and mass confirmation was performed on post-PDA eluent using a Micromass Quattro Ultima mass spectrometer with MassLynx 4.1 (Waters). The LLOQ ranged from 10 to 30 ng/mL (depending on sample background) to an upper limit of 50  $\mu\text{g}/\text{mL}$ . RTD-2 (10  $\mu\text{g}/\text{mL}$ ) was used as an internal standard. Intra- and interassay precision (% coefficient of variation [CV]) was  $\leq 3\%$ , and intra- and interassay accuracy (% relative error) was  $\leq 5\%$ .

**Pharmacokinetic analysis.** Noncompartmental analysis (NCA) was performed using Phoenix WinNonlin (version 8.3.1; Certara USA, Inc., Princeton, NJ) to determine the PK parameters in mice, rats, cynomolgus monkeys, and a vervet. Nominal sampling times were used in the analysis, and data below the lower limit of quantification of the assay were excluded from the analysis. The maximum plasma concentration ( $C_{\text{max}}$ ) was determined from visual inspection of the data. In addition, the following parameters were calculated: terminal elimination rate constant ( $\lambda_z$ ), area under the curve extrapolated to infinity ( $\text{AUC}_{0-\infty}$ ), area under the curve to dosing interval ( $\text{AUC}_\tau$ ), mean residence time (MRT), clearance

(CL), and volume of distribution at steady state ( $V_{ss}$ ). AUC was calculated using the linear up, log down method, and the  $\lambda_z$  was calculated using up to the last four data points of the log-linear terminal phase of the concentration-time profile. Due to sparsely sampled data in mice and rats, the sparse sampling calculation methodology in Phoenix WinNonlin was used, which generated a single estimate without standard error for all parameters except  $C_{max}$ . For rats and cynomolgus monkeys, all parameters were calculated using sampling times relative to the beginning of the i.v. infusion.

**Dose proportionality.** Dose proportionality of  $C_{max}$  and  $AUC_{0-\infty}$  was evaluated in cynomolgus monkeys administered a single i.v. dose of RTD-1 ranging from 0.3 to 15 mg/kg using a natural log-transformed power model (36). Dose proportionality was concluded if the slope and the corresponding 95% confidence interval of the linear regression included 1.

**Interspecies allometric scaling.** Single-dose PK data from mice, rats, cynomolgus monkeys, and a vervet was used to predict human PK parameters using simple allometry. The relationship between CL or  $V_{ss}$  was obtained from the NCA, and the body weight was described using the following equation  $Y = a \times BW^b$ , where  $Y$  is the PK parameter (e.g., CL or  $V_{ss}$ ),  $BW$  is the body weight of the species,  $a$  is an allometric coefficient, and  $b$  is an allometric exponent (33, 37). Linear regression was performed on log-transformed data. The predicted HED was calculated based on the allometrically scaled CL by use of the following equation:  $\text{dose} = CL \times AUC_{0-\infty}$ . The corresponding average  $AUC_T$  and  $AUC_{0-\infty}$  at NOAEL and LOAEL, respectively, were used to convert the doses at NOAEL and LOAEL in preclinical animals to HED.

**Biodistribution  $^{14}\text{C}$ -radiolabeled RTD-1 in female rats.** Five Sprague-Dawley rats (195 to 200 g body weight) with jugular vein catheters (JVC) were each injected with 200  $\mu\text{l}$  of 5 mg/mL RTD-1 in saline containing  $\sim 4$  million cpm of [ $^{14}\text{C}$ ]RTD-1. The [ $^{14}\text{C}$ ]RTD-1 was created by substituting the natural glycine residue on position 1 of the cyclic peptide with a  $^{14}\text{C}$ -labeled glycine. The JVC line was cleaned with 70% isopropyl alcohol, and the line plug was removed. A new 25-gauge blunt needle with a 1-mL syringe containing injectable solutions was used for each injection. The JVC line was first cleared with 100  $\mu\text{L}$  saline, followed by the RTD-1 solution, and then cleared with an additional 100  $\mu\text{L}$  of saline. Tissues and organs were harvested into separate vials and weighed. Small organs such as lymph nodes, kidneys, and heart/lungs were processed whole. Large organs (e.g., liver, muscles, subcutaneous fat pads) were sampled from representative areas or those of interest (e.g., subcutis at the injection site). Organs were then dissolved in 2 mL Solvable (Perkin Elmer 6NE9100) for up to 1 g of tissue. For a large section of skin and other organs, 4 or 6 mL was added. Vials were incubated in a 60°C water bath for 18 to 22 h and then removed and allowed to cool to room temperature. Two milliliters of dissolved tissue was added to a fresh scintillation tube for color correction with 100  $\mu\text{L}$  of 0.1 M EDTA and  $2 \times 100 \mu\text{L}$  30% hydrogen peroxide. Samples were allowed to stand at room temperature for 1 h, incubated in a 37°C incubator for 1 h, and then incubated in a 60°C water bath for 1 h. If necessary to prevent boiling over, samples were removed from the heat source temporarily before continuing. Samples were cooled before 10 mL of Ultima Gold (Perkin Elmer 6013321) was added to each vial, and then contents were mixed and allowed to stand in the dark at 22°C for 1 h. Scintillation counting was an average of two 1-min counts using a Packard Tri-Carb 2100TR scintillation counter. Urine was collected over 1 h or 24 h after i.v. infusion, and 500  $\mu\text{L}$  was added to a scintillation vial processed as described above for scintillation counting. The stomach and its content were dissolved with 6 mL of Solvable and processed as for other tissues. The duodenum, jejunum, and ileum were flushed with saline to remove luminal contents, and then the tissues were processed with Solvable as described above. The large intestine was opened lengthwise to remove fecal content, rinsed with saline to remove the remaining luminal contents, and then processed as described above. Feces were collected, transferred into a 500-mL plastic cup, and treated with 50 mL of 7% sodium hypochlorite and allowed to react for 1 h at 22°C, followed by 1 h in a 60°C water bath. Two milliliters of the resulting suspension was transferred to a scintillation vial and mixed with 10 mL of scintillation fluid. The contents were mixed and allowed to stand for 1 h before scintillation counting.

**Safety.** Evaluation of safety in rats and cynomolgus monkeys was based on clinical observations, survival, body weight, food consumption, clinical pathology (hematology, clinical chemistry, and coagulation), urinalysis, ophthalmology, macroscopic findings at necropsy, and microscopic histopathology and is described in detail in the supplemental material. The schedule of assessments for these studies is summarized in Table S2.

**Statistical analysis.** Statistical analysis of the PK data was performed with GraphPad Prism version 9.1.2 (GraphPad Software, Inc., San Diego, CA). The Shapiro-Wilk test was used to check for normality. One-way analysis of variance (ANOVA) with Bonferroni's multiple-comparison test was performed to compare  $C_{max}$  values across doses (5, 10, and 20 mg/kg) in rats, and  $\lambda_z$ , AUC,  $C_{max}$ , CL, and  $V_{ss}$  values across doses (5, 10, and 15 mg/kg) in cynomolgus monkeys. An unpaired  $t$  test was used to compare PK parameters ( $\lambda_z$ , AUC,  $C_{max}$ , CL, and  $V_{ss}$ ) between different days (day 1 versus day 10) within each dosing group and between sexes. Statistical analyses of safety data were performed using SAS 9.4, considering a 95% statistical significance. Differences in body weight, change in body weight, and clinical pathology (hematology, serum chemistry, coagulation) were compared between each dose group using the Kruskal-Wallis test with Dunn's multiple comparison test. The data analysis was performed independently for each sex.

## SUPPLEMENTAL MATERIAL

Supplemental material is available online only.

**SUPPLEMENTAL FILE 1**, PDF file, 0.2 MB.

## REFERENCES

- Gupta A, Madhavan MV, Sehgal K, Nair N, Mahajan S, Sehrawat TS, Bikdeli B, Ahluwalia N, Ausiello JC, Wan EY, Freedberg DE, Kirtane AJ, Parikh SA, Maurer MS, Nordvig AS, Accili D, Bathon JM, Mohan S, Bauer KA, Leon MB, Krumholz HM, Uriel N, Mehra MR, Elkind MSV, Stone GW, Schwartz A, Ho DD, Bilezikian

- JP, Landry DW. 2020. Extrapulmonary manifestations of COVID-19. *Nat Med* 26:1017–1032. <https://doi.org/10.1038/s41591-020-0968-3>.
2. Wohlford-Lenane CL, Meyerholz DK, Perlman S, Zhou H, Tran D, Selsted ME, McCray PB. 2009. Rhesus theta-defensin prevents death in a mouse model of severe acute respiratory syndrome coronavirus pulmonary disease. *J Virol* 83:11385–11390. <https://doi.org/10.1128/JVI.01363-09>.
  3. Jayne JG, Bensman TJ, Schaal JB, Park AY, Kimura E, Tran D, Selsted ME, Beringer PM. 2018. Rhesus  $\theta$ -defensin-1 attenuates endotoxin-induced acute lung injury by inhibiting proinflammatory cytokines and neutrophil recruitment. *Am J Respir Cell Mol Biol* 58:310–319. <https://doi.org/10.1165/rcmb.2016-04280C>.
  4. Zhang W, Zhao Y, Zhang F, Wang Q, Li T, Liu Z, Wang J, Qin Y, Zhang X, Yan X, Zeng X, Zhang S. 2020. The use of anti-inflammatory drugs in the treatment of people with severe coronavirus disease 2019 (COVID-19): the experience of clinical immunologists from China. *Clin Immunol* 214: 108393. <https://doi.org/10.1016/j.clim.2020.108393>.
  5. Chen L, Liu H, Liu W, Liu J, Liu K, Shang J, Deng Y, Wei S. 2020. Analysis of clinical features of 29 patients with 2019 novel coronavirus pneumonia. *Zhonghua Jie He He Hu Xi Za Zhi* 43:203–208. (In Chinese.). <https://doi.org/10.3760/cma.j.issn.1001-0939.2020.03.013>.
  6. Huang C, Wang Y, Li X, Ren L, Zhao J, Hu Y, Zhang L, Fan G, Xu J, Gu X, Cheng Z, Yu T, Xia J, Wei Y, Wu W, Xie X, Yin W, Li H, Liu M, Xiao Y, Gao H, Guo L, Xie J, Wang G, Jiang R, Gao Z, Jin Q, Wang J, Cao B. 2020. Clinical features of patients infected with 2019 novel coronavirus in Wuhan, China. *Lancet* 395:497–506. [https://doi.org/10.1016/S0140-6736\(20\)30183-5](https://doi.org/10.1016/S0140-6736(20)30183-5).
  7. Ruan Q, Yang K, Wang W, Jiang L, Song J. 2020. Clinical predictors of mortality due to COVID-19 based on an analysis of data of 150 patients from Wuhan, China. *Intensive Care Med* 46:846–848. <https://doi.org/10.1007/s00134-020-05991-x>.
  8. RECOVERY Collaborative Group, Horby P, Lim WS, Emberson JR, Mafham M, Bell JL, Linsell L, Staplin N, Brightling C, Ustianowski A, Elmahi E, Prudon B, Green C, Felton T, Chadwick D, Rege K, Fegan C, Chappell LC, Faust SN, Jaki T, Jeffery K, Montgomery A, Rowan K, Juszczak E, Baillie JK, Haynes R, Landray MJ. 2021. Dexamethasone in hospitalized patients with Covid-19. *N Engl J Med* 384:693–704. <https://doi.org/10.1056/NEJMoa2021436>.
  9. Tran D, Tran P, Roberts K, Osapay G, Schaal J, Ouellette A, Selsted ME. 2008. Microbicidal properties and cytotoxic selectivity of rhesus macaque theta defensins. *Antimicrob Agents Chemother* 52:944–953. <https://doi.org/10.1128/AAC.01090-07>.
  10. Seidel A, Ye Y, De Armas LR, Soto M, Yarosh W, Marcsisin RA, Tran D, Selsted ME, Camerini D. 2010. Cyclic and acyclic defensins inhibit human immunodeficiency virus type-1 replication by different mechanisms. *PLoS One* 5:e9737. <https://doi.org/10.1371/journal.pone.0009737>.
  11. Bensman TJ, Jayne JG, Sun M, Kimura E, Meinert J, Wang JC, Schaal JB, Tran D, Rao AP, Akbari O, Selsted ME, Beringer PM. 2017. Efficacy of rhesus theta-defensin-1 in experimental models of *Pseudomonas aeruginosa* lung infection and inflammation. *Antimicrob Agents Chemother* 61: e00154-17. <https://doi.org/10.1128/AAC.00154-17>.
  12. Basso V, Tran DQ, Schaal JB, Tran P, Eriguchi Y, Ngole D, Cabebe AE, Park A, Beringer PM, Ouellette AJ, Selsted ME. 2019. Rhesus theta defensin 1 promotes long term relapse in systemic candidiasis by host directed mechanisms. *Sci Rep* 9:14. <https://doi.org/10.1038/s41598-019-53402-z>.
  13. Tongaonkar P, Trinh KK, Schaal JB, Tran D, Gulko PS, Ouellette AJ, Selsted ME. 2015. Rhesus macaque  $\theta$ -defensin RTD-1 inhibits proinflammatory cytokine secretion and gene expression by inhibiting the activation of NF- $\kappa$ B and MAPK pathways. *J Leukoc Biol* 98:1061–1070. <https://doi.org/10.1189/jlb.3A0315-102R>.
  14. Schaal JB, Marezky T, Tran DQ, Tran PA, Tongaonkar P, Blobel CP, Ouellette AJ, Selsted ME. 2018. Macrocyclic  $\theta$ -defensins suppress tumor necrosis factor- $\alpha$  (TNF- $\alpha$ ) shedding by inhibition of TNF- $\alpha$ -converting enzyme. *J Biol Chem* 293:2725–2734. <https://doi.org/10.1074/jbc.RA117.000793>.
  15. Schaal JB, Tran D, Tran P, Osapay G, Trinh K, Roberts KD, Brasky KM, Tongaonkar P, Ouellette AJ, Selsted ME. 2012. Rhesus macaque theta defensins suppress inflammatory cytokines and enhance survival in mouse models of bacteremic sepsis. *PLoS One* 7:e51337. <https://doi.org/10.1371/journal.pone.0051337>.
  16. Tongaonkar P, Punj V, Subramanian A, Tran DQ, Trinh KK, Schaal JB, Laragione T, Ouellette AJ, Gulko PS, Selsted ME. 2019. RTD-1 therapeutically normalizes synovial gene signatures in rat autoimmune arthritis and suppresses proinflammatory mediators in RA synovial fibroblasts. *Physiol Genomics* 51:657–667. <https://doi.org/10.1152/physiolgenomics.00066.2019>.
  17. Schaal JB, Tran DQ, Subramanian A, Patel R, Laragione T, Roberts KD, Trinh K, Tongaonkar P, Tran PA, Minond D, Fields GB, Beringer P, Ouellette AJ, Gulko PS, Selsted ME. 2017. Suppression and resolution of autoimmune arthritis by rhesus  $\theta$ -defensin-1, an immunomodulatory macrocyclic peptide. *PLoS One* 12:e0187868. <https://doi.org/10.1371/journal.pone.0187868>.
  18. Petterino C, Argentino-Storino A. 2006. Clinical chemistry and haematology historical data in control Sprague-Dawley rats from pre-clinical toxicity studies. *Exp Toxicol Pathol* 57:213–219. <https://doi.org/10.1016/j.etp.2005.10.002>.
  19. FDA. 2005. Guidance for industry estimating the maximum safe starting dose in initial clinical trials for therapeutics in adult healthy volunteers. Food and Drug Administration, Rockville, MD.
  20. Schuurman HJ, Smith HT. 2005. Reference values for clinical chemistry and clinical hematology parameters in cynomolgus monkeys. *Xenotransplantation* 12:72–75. <https://doi.org/10.1111/j.1399-3089.2004.00186.x>.
  21. Catanzaro M, Fagiani F, Racchi M, Corsini E, Govoni S, Lanni C. 2020. Immune response in COVID-19: addressing a pharmacological challenge by targeting pathways triggered by SARS-CoV-2. *Signal Transduct Target Ther* 5:84. <https://doi.org/10.1038/s41392-020-0191-1>.
  22. Merad M, Martin JC. 2020. Pathological inflammation in patients with COVID-19: a key role for monocytes and macrophages. *Nat Rev Immunol* 20:355–362. <https://doi.org/10.1038/s41577-020-0331-4>.
  23. Chen T, Mager DE, Kagan L. 2013. Interspecies modeling and prediction of human xenatide pharmacokinetics. *Pharm Res* 30:751–760. <https://doi.org/10.1007/s11095-012-0917-z>.
  24. Kagan L, Abraham AK, Harrold JM, Mager DE. 2010. Interspecies scaling of receptor-mediated pharmacokinetics and pharmacodynamics of type I interferons. *Pharm Res* 27:920–932. <https://doi.org/10.1007/s11095-010-0098-6>.
  25. Tanaka C, Kawai R, Rowland M. 2000. Dose-dependent pharmacokinetics of cyclosporin A in rats: events in tissues. *Drug Metab Dispos* 28:582–589.
  26. Kato M, Kamiyama H, Okazaki A, Kumaki K, Kato Y, Sugiyama Y. 1997. Mechanism for the nonlinear pharmacokinetics of erythropoietin in rats. *J Pharmacol Exp Ther* 283:520–527.
  27. Di L. 2015. Strategic approaches to optimizing peptide ADME properties. *AAPS J* 17:134–143. <https://doi.org/10.1208/s12248-014-9687-3>.
  28. Diao L, Meibohm B. 2013. Pharmacokinetics and pharmacokinetic-pharmacodynamic correlations of therapeutic peptides. *Clin Pharmacokinet* 52:855–868. <https://doi.org/10.1007/s40262-013-0079-0>.
  29. Huh Y, Smith DE, Feng MR. 2011. Interspecies scaling and prediction of human clearance: comparison of small- and macro-molecule drugs. *Xenobiotica* 41:972–987. <https://doi.org/10.3109/00498254.2011.598582>.
  30. Mahmood I, Balian JD. 1996. Interspecies scaling: predicting clearance of drugs in humans. Three different approaches. *Xenobiotica* 26:887–895. <https://doi.org/10.3109/00498259609052491>.
  31. Mordenti J, Chen SA, Moore JA, Ferraiolo BL, Green JD. 1991. Interspecies scaling of clearance and volume of distribution data for five therapeutic proteins. *Pharm Res* 8:1351–1359. <https://doi.org/10.1023/a:1015836720294>.
  32. FDA. 2005. Estimating the maximum safe starting dose in initial clinical trials for therapeutics in adult healthy volunteers. Food and Drug Administration, Rockville, MD.
  33. Caldwell GW, Masucci JA, Yan Z, Hageman W. 2004. Allometric scaling of pharmacokinetic parameters in drug discovery: can human CL, V<sub>s</sub> and t<sub>1/2</sub> be predicted from in-vivo rat data? *Eur J Drug Metab Pharmacokinet* 29:133–143. <https://doi.org/10.1007/BF03190588>.
  34. Feng Z, Yu Q, Yao S, Luo L, Zhou W, Mao X, Li J, Duan J, Yan Z, Yang M, Tan H, Ma M, Li T, Yi D, Mi Z, Zhao H, Jiang Y, He Z, Li H, Nie W, Liu Y, Zhao J, Luo M, Liu X, Rong P, Wang W. 2020. Early prediction of disease progression in COVID-19 pneumonia patients with chest CT and clinical characteristics. *Nat Commun* 11:4968. <https://doi.org/10.1038/s41467-020-18786-x>.
  35. McElvaney OJ, McEvoy NL, McElvaney OF, Carroll TP, Murphy MP, Dunlea DM, Ni Choileáin O, Clarke J, O'Connor E, Hogan G. 2020. Characterization of the inflammatory response to severe COVID-19 illness. *Am J Respir Crit Care Med* 202:812–821. <https://doi.org/10.1164/rccm.202005-1583OC>.
  36. Gough K, Hutchison M, Keene O, Byrom B, Ellis S, Lacey L, McKellar J. 1995. Assessment of dose proportionality: report from the statisticians in the pharmaceutical industry/pharmacokinetics UK joint working party. *Drug Inf J* 29:1039–1048. <https://doi.org/10.1177/009286159502900324>.
  37. Amantana A, Chen Y, Tyavanagimatt SR, Jones KF, Jordan R, Chinsangaram J, Bolken TC, Leeds JM, Hruby DE. 2013. Pharmacokinetics and interspecies allometric scaling of ST-246, an oral antiviral therapeutic for treatment of orthopoxvirus infection. *PLoS One* 8:e61514. <https://doi.org/10.1371/journal.pone.0061514>.